
Development of duplex TaqMan-based real-time PCR assay for the simultaneous detection of *Perkinsus olseni* and *P. chesapeaki* in host Manila clam tissue samples

Itoïz Sarah ¹, Perennou Morgan ¹, Mouronville Clara ^{1,2}, Derelle Evelyne ¹, Le Goïc Nelly ¹, Bidault Adeline ^{1,5}, De Montaudouin Xavier ³, Arzul Isabelle ⁴, Soudant Philippe ^{1,*}, Chambouvet Aurélie ^{1,*}

¹ Univ Brest, CNRS, IRD, Ifremer, LEMAR, F-29280 Plouzané, France

² EPHE, PSL Research University, UPVD, CNRS, USR 3278 CRIOBE, Perpignan F-66360, France

³ Univ. Bordeaux, CNRS, EPOC, EPHE, UMR 5805, Station Marine, F-33120 Arcachon, France

⁴ IFREMER, Laboratory of Genetics and Pathology, Av de Mus de Loup-17390, La Tremblade, France

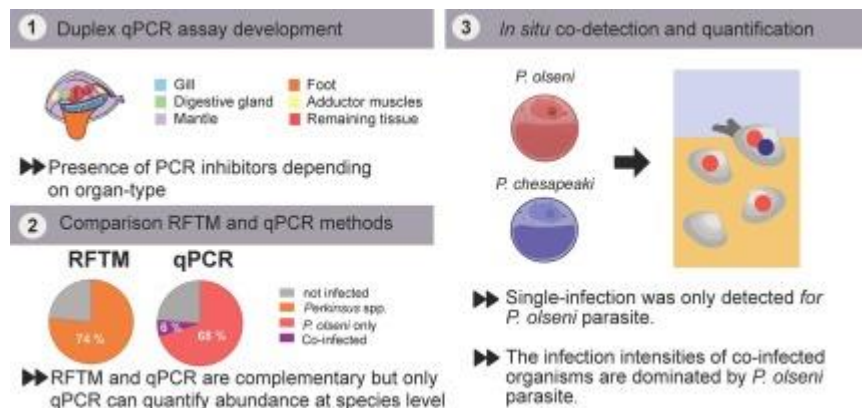
⁵ Univ Brest, CNRS, IRD, Ifremer, LEMAR, F-29280 Plouzané, France

* Corresponding authors : Philippe Soudant, email address : philippe.soudant@univ-brest.fr ; Aurélie Chambouvet, email address : aurelie.chambouvet@univ-brest.fr

Abstract :

The aetiological agent *Perkinsus olseni* is globally recognised as a major threat for shellfish production considering its wide geographical distribution across Asia, Europe, Australia and South America. Another species, *Perkinsus chesapeaki*, which has never been known to be associated with significant mortality events, was recently detected along French coasts infecting clam populations sporadically in association with *P. olseni*. Identifying potential cryptic infections affecting *Ruditapes philippinarum* is essential to develop appropriate host resource management strategies. Here, we developed a molecular method based on duplex real-time quantitative PCR for the simultaneous detection of these two parasites, *P. olseni* and *P. chesapeaki*, in the different clam tissues: gills, digestive gland, foot, mantle, adductor muscle and the rest of the soft body. We firstly checked the presence of possible PCR inhibitors in host tissue samples. The qPCR reactions were inhibited depending on the nature of the host organ. The mantle and the rest of the soft body have a high inhibitory effect from threshold of host gDNA concentration of 2 ng.µL⁻¹, the adductor muscle and the foot have an intermediate inhibition of 5 ng.µL⁻¹, and the gills and digestive gland do not show any inhibition of the qPCR reaction even at the highest host gDNA concentration of 20 ng.µL⁻¹. Then, using the gills as a template, the suitability of the molecular technique was checked in comparison with the Ray's Fluid Thioglycolate Medium methodology recommended by the World Organisation for Animal Health. The duplex qPCR method brought new insights and unveiled cryptic infections as the co-occurrence of *P. olseni* and *P. chesapeaki* from in situ tissue samples in contrast to the RFTM diagnosis. The development of this duplex qPCR method is a fundamental work to monitor in situ co-infections that will lead to optimised resource management and conservation strategies to deal with emerging diseases.

Graphical abstract



Highlights

► Duplex qPCR is a suitable method to detect simultaneously *P. olseni* and *P. chesapeakei* within Manila clam. ► PCR inhibitor compounds are present in Manila clam gDNA depending on the organ-type. ► For each organ, a threshold concentration of host gDNA is needed for good use of PCR and qPCR. ► Duplex qPCR results are correlated with those obtained by standard thioglycolate method. ► In Arcachon bay, the prevalence of co-infection is low (6 %) and the intensity of infection is dominated by *P. olseni*. ► Single-infection is only detected for *P. olseni* parasite.

Keywords : Alveolata, Co-infection, Molluscs, Inhibitory effect, *Ruditapes philippinarum*, qPCR

51 **1. Introduction**

52 Manila clam, *Ruditapes philippinarum*, is extensively cultured worldwide with 4.23
53 million tons harvested in 2017 representing 25% of global bivalve production (FAO,
54 2018). Introduced in Europe in the 1970s (Flassch and Leborgne, 1994) for aquaculture
55 purposes, this bivalve is currently the third most important bivalve produced in Europe
56 after mussels and oysters (European Commission - DG for health and food safety, 2018).
57 However, this valuable economic resource is regularly threatened by infectious diseases
58 caused by a wide variety of pathogenic agents including bacteria, virus, and protists,
59 leading to mortality events with significant economic consequences (Allam *et al.*, 2002;
60 Jenkins *et al.*, 2013; Azevedo, 1989). It is today widely accepted that coastal ecosystems
61 are threatened by an unprecedented environmental transformation and the influence of
62 these changes on disease epizootics is now a major scientific issue to tackle. These
63 drastic changes, related to multifactorial anthropogenic consequences, might alter the
64 host-pathogen balance illustrated by an increase in prevalence and severity of disease
65 outbreaks (Harvell, 2002; Ward and Lafferty, 2004). Perkinsosis is one of the most
66 widespread marine diseases globally in commercially important marine molluscs
67 including oysters, clams and abalones. Two main parasites, *Perkinsus marinus* and
68 *Perkinsus olseni*, identified as the infectious agents of perkinsosis, have been classified as
69 notifiable pathogens in the Organisation for Animal Health (OIE)-list diseases since 2006
70 (OIE, 2019a). *P. marinus* is responsible for extensive oyster mortalities mostly in the Gulf
71 of Mexico and in the Chesapeake Bay (Mackin *et al.*, 1950; Mackin, 1951; Burreson and
72 Andrews, 1988; Burreson *et al.*, 1994; Andrews, 1996). *P. olseni*, which has a broad
73 geographic distribution (e.g. Europe: Arzul *et al.*, 2012; Azevedo, 1989; Australia: Goggin
74 and Lester, 1995; Asia: Hamaguchi *et al.*, 1998; Park and Choi, 2001; Shamal *et al.*, 2018;
75 America: Pagenkopp Lohan *et al.*, 2018), is often associated with clam mortalities in Asia
76 (Park and Choi, 2001; Nam *et al.*, 2018) and in Europe (Da Ros and Canzonier, 1985;
77 Ruano and Cachola, 1986; Azevedo, 1989; Pretto *et al.*, 2014), and abalone mortality in
78 Australia (Goggin and Lester, 1995). Even when infection by *Perkinsus* species does not
79 directly produce host death it can induce sublethal effects resulting in reduced growth
80 and reproductive activity and a general decrease in host health which favours secondary
81 opportunistic infections (Tall *et al.*, 1999; Dittman *et al.*, 2001; Montes *et al.*, 2001; Lee *et*
82 *al.*, 2001).

83 The advent of molecular methods brought new insights in species definition and helped
84 unravel cryptic infections across various fields including marine environments
85 (Putaporntip *et al.*, 2009; Chambouvet *et al.*, 2015). Recently, using a combination of
86 culture methodology and conventional PCR, co-occurrences of two *Perkinsus* species
87 within the same host tissue samples have been reported (e.g. Reece *et al.*, 2008, Coss *et*
88 *al.*, 2001, Takahashi *et al.*, 2009). In Europe, two *Perkinsus* species, *P. olseni* and *P.*
89 *chesapeakei*, were identified sporadically co-infecting the native grooved carpet shell
90 clam, *Ruditapes decussatus*, from Leucate lagoon (Arzul *et al.*, 2012) and the exotic
91 Manila clam, *R. philippinarum*, from Galicia (NW Spain)(Ramilo *et al.*, 2016).
92 Hypothetically, *P. olseni* and *P. chesapeakei* were accidentally introduced with their
93 vector, the Manila clam *R. philippinarum* from Asia and the soft-shell clam, *Mya arenaria*,
94 or the hard clam, *Mercenaria mercenaria*, from U.S.A., respectively (Arzul *et al.*, 2012). As
95 opposed to *P. olseni*, *P. chesapeakei* has never been obviously associated with a mass
96 mortality event despite some suspicions it may cause mortality in the stout razor clam,
97 *Tagelus plebeius*, in the U.S.A. (Bushek *et al.*, 2008). Although these two parasites are
98 detected along the European Atlantic coastline, their distribution, prevalence and impact
99 on infection outcome remain an important scientific gap that urgently needs to be
100 fulfilled because the 'one parasite-one disease' paradigm is now outdated. Indeed, today,
101 disease outcomes frequently reflect an interaction network including numerous
102 different pathogens within a single host (Bass *et al.*, 2019).

103 The standard methodology for *Perkinsus* spp. quantification, recommended by the O.I.E.,
104 is the incubation of infected host tissues samples in Ray's fluid thioglycolate medium
105 (RFTM) followed by alkaline digestion with NaOH and blue-black staining of the
106 infectious parasitic cells with Lugol's iodine (Choi *et al.*, 1989; OIE, 2019b; Ray, 1952).
107 The RFTM methodology, which is easy to perform, inexpensive and sensitive to a very
108 low infection intensity, is now widely used (Choi *et al.*, 1989; Bushek *et al.*, 1994). In
109 parallel, classical haematoxylin and eosin staining histology methodology, also
110 recommended by the OIE, is very useful to visualise lesions and parasite distribution in
111 tissues even if it is time-consuming and less sensitive (OIE, 2019b). It allows a
112 qualitative detection of parasites from *Perkinsus* genus within the different tissue
113 samples. However, these two methods do not adequately identify the parasite species or
114 the presence of co-infection by parasites of the same genus. These two non-specific
115 methods should now be complemented with molecular tools for quantitative and

116 qualitative detection (Almeida *et al.*, 1999; Novoa *et al.*, 2002; Audemard *et al.*, 2008;
117 Balseiro *et al.*, 2010). Molecular based methods, e.g. conventional PCR and RFLP
118 (Restriction Fragment Length Polymorphic) assays, were used to detect the presence or
119 absence of the genetic signature of the different *Perkinsus* species in culture or in host
120 tissue samples (Takahashi *et al.*, 2009; Arzul *et al.*, 2012; Ramilo *et al.*, 2016). Recently,
121 real-time quantitative PCR (qPCR) methodology was developed to quantify the
122 abundance and the prevalence of different *Perkinsus* species within host tissue samples
123 and / or in environmental samples (Audemard *et al.*, 2004; Umeda and Yoshinaga, 2012;
124 Ríos *et al.*, 2020). In 2018, Cui *et al.* highlighted for the first time, using qPCR method, a
125 seasonal pattern between *P. olseni* and *P. beihaiensis* infecting the clam *Soletellina acuta*
126 in China (Cui *et al.*, 2018). Such results highlighted that cryptic infection by different
127 *Perkinsus* species, usually unnoticed by classical methodology, can play a key role in the
128 infection process and therefore on disease outcomes.

129 The qPCR methodology is an accurate and sensitive tool which should be more widely
130 used because it is now clear that co-infection between *Perkinsus* species might be more
131 frequent than expected. However, a major drawback for qPCR assays is the presence of
132 potential PCR inhibitors that can hinder parasite quantification. These inhibitor
133 compounds, usually co-extracted during the nucleic acid extraction, are currently
134 prevalent in shellfish tissue (Hohweyer *et al.*, 2013). To avoid strong PCR inhibition, the
135 dilution of inhibited samples provides a rapid and simple way to overcome this problem
136 (Renault *et al.*, 2000). This easy method was performed to rule out false negatives but
137 may dilute the number of targeted molecules below the limit of the detection method
138 (Batista *et al.*, 2007).

139 Given that *P. olseni* is not systematically associated with mortality, the detection and
140 quantification of another infectious agent co-infecting same hosts could lead to a better
141 comprehension of the disease outcome. The aim of this study was to develop a duplex
142 TaqMan-based real-time PCR assay to quantify the two *Perkinsus* species, *P. olseni* and *P.*
143 *chesapeakei*, in Manila clam host tissues samples and thus detect and monitor specifically
144 the co-infection of *P. olseni* and *P. chesapeakei* in the valuable population of Manila clams
145 from different locations.

146

147

148

149

150 **2. Material & methods**

151

152 **2.1. Manila clams sampling**

153 Clams were collected during a sampling campaign in Arcachon bay (SW France, Atlantic
154 coast, 44°41'60" N;1°10' W) the 7th and 8th of November 2018 (Itoiz *et al.*, in prep). A
155 total of 55 Manila clams, *Ruditapes philippinarum*, were collected from the station
156 Lanton (Figure S1; Table S1). Arcachon bay is a mesotidal lagoon of 180 km² where
157 intertidal mudflat macrofauna is mainly dominated by *R. philippinarum*, which could
158 represent up to 90% of the total biomass (Bertignac *et al.*, 2001).

159 Of the 55 clams sampled, fifty were dissected for RFTM and molecular assays. Briefly,
160 clams were opened on ice and one gill was weighed and incubated in RFTM
161 supplemented with antibiotics (penicillin 66 µg.mL⁻¹ and streptomycin 32 µg.mL⁻¹) and
162 antimycotic (nystatin 0.04 mg.mL⁻¹), with subsequent *Perkinsus* quantification according
163 to Choi *et al.* (1989). The rest of each oyster was dissected into six compartments: the
164 second gill, the digestive gland, the mantle, the adductor muscle, the foot and the
165 remaining tissue. Each organ was weighed and preserved separately in 80% ethanol at
166 4°C until further molecular analysis. Shells were measured and weighed. Five clams
167 were kept in a 40L tank of filtered (0.2 µm) sea water at 15°C for 10 days before using
168 them for establishing *P. olsenii* and *P. chesapeaki* cultures.

169

170 **2.2. Ray's fluid thioglycolate medium (RFTM)**

171 Body-burden assays were conducted following the RFTM method as recommended by
172 the O.I.E. (Ray, 1952; Choi *et al.*, 1989; OIE, 2019b). Briefly, after incubation in RFTM in
173 the dark for five days at room temperature, allowing the enlargement of trophozoites
174 (hypnospore formation) (Ray, 1952), gill tissue samples were digested with 2M NaOH
175 solution for 3 h at 60 °C preserving the hypnospore cell structure (Choi *et al.*, 1989).
176 Hypnospores were then stained with a Lugol's iodine solution (4 %), and counted in a

177 Nageotte chamber (ten lines in triplicate) under a microscope (Leica DM-IRB; x10
178 magnification). The counting results were expressed as the number of hypospores per
179 gram of wet tissue.

180

181 **2.3. *In vitro* culture of monoclonal strains of *P. olseni* and *P. chesapeaki***

182 The five preserved Manila clams were used to established cultures following a simplified
183 protocol from Casas *et al.* (2002a). In short, gill tissue samples were excised and
184 decontaminated with five successive baths of antibiotic solution (concentrations per L⁻¹:
185 400 000 U ampicillin - 0.4 g streptomycin sulphate (Sigma-Aldrich), 0.4 g kanamycin
186 (Sigma-Aldrich), 0.2 g gentamycin (Sigma-Aldrich)) and baths of sterile sea water. Gill
187 samples were incubated in *Perkinsus* medium broth (ATCC medium 1886)
188 supplemented with antimycotic (40 U.mL⁻¹ nystatin, Sigma-Aldrich) and antibiotics (100
189 U.mL⁻¹ penicillin and 0.1 mg.mL⁻¹ streptomycin, Sigma-Aldrich) at 25°C for 10-15 days to
190 allow trophozoites to proliferate. Five cultures were initiated from the five gills that
191 were initially incubated. To characterise the *Perkinsus* species, the five cultures were
192 sampled after two weeks of incubation for molecular analysis based on PCR (using
193 primers ITS-85/ITS-750, Casas *et al.*, 2002b) and amplicon sequencing. Monoclonal
194 cultures of *P. olseni* and *P. chesapeaki* were established using two of these cultures. Briefly,
195 using the agar-based method developed by Cold *et al.* (2016), initial cultures of *P. olseni* and
196 *P. chesapeaki* were diluted at 2,000 cells.mL⁻¹ in *Perkinsus* medium broth (ATCC medium
197 1886) before plating onto solid medium (*Perkinsus* medium broth [ATCC medium 1886]
198 implemented with 0.75 % agar). Agar plates were incubated at 25°C until the first visible
199 colonies appeared. Each colony was assessed using an inverted light microscope and sub-
200 cloned twice using the same methodology before seeding into liquid *Perkinsus* broth medium
201 (ATCC medium 1886). Two monoclonal strain cultures were selected to establish *P. olseni*
202 and *P. chesapeaki* plasmid-standard curves (Figure S2).

203

204 **2.4. DNA extraction**

205 The genomic DNA (gDNA) of the six organs (gill, digestive gland, mantle, adductor
206 muscle, foot and the remaining tissue samples) was extracted using CTAB-based DNA
207 extraction method adapted from Winnepenninckx *et al.* (1993). Organ tissues were

208 transferred in bead beating tubes containing three different bead sizes (2.8 mm, 1.4 mm
209 and 0.1 mm of diameter, Ozyme) with 1 mL of CTAB extraction buffer (2 % CTAB, 100
210 mM TrisHCl pH=8.0, 20 mM EDTA, 1.4 mM NaCl) and placed into cooling rack. Samples
211 were then ground and homogenized following two bead beating cycles (45 seconds of
212 bead beating at 6 m. s⁻¹ following by 20 seconds stopped) using the FastPrep-24 5G (MP
213 Biomedicals). After this step, β-mercaptoethanol (0.2 %) and proteinase K (0.1 mg.mL⁻¹)
214 were then added in each tube and samples were incubated for 30 min at 60°C. The one
215 exception to this was foot tissue samples, which were incubated for 12 hours due to this
216 tissue's dense muscular structure. Lysates were mixed in chloroform/isoamylalcohol
217 (24:1, v/v) and emulsified before spinning for 10 min at 18.000 g rpm in a cooled
218 microcentrifuge (4°C). This step was repeated twice for the foot tissue samples. Aqueous
219 phases were treated with RNase solution (10mg.mL⁻¹, Sigma-Aldrich) for 30 minutes at
220 37°C, and then DNA was precipitated with cold 100% isopropanol overnight at 4°C. DNA
221 was pelleted and rinsed with two successive washes of cold 70% ethanol. The DNA
222 pellets were then dried at room temperature until complete ethanol evaporation and
223 resuspended in 300 µl of pure molecular grade water (Corning). After DNA
224 quantification using the Qubit dsDNA HS assay kit (Invitrogen), the DNA samples were
225 stored at -20 °C until further downstream processing.

226

227 **2.5. Duplex qPCR assay development**

228

229 **2.5.1. Targeted amplification of the ITS sequences of two *Perkinsus*** 230 **monoclonal strains**

231 PCR assays were performed using *Perkinsus*-genus specific primers ITS-85/ITS-750
232 (Casas *et al.*, 2002b) targeting the sequences of rDNA Internal Transcribed Spacer (ITS)
233 regions. All PCR reactions were performed (25 µL final volume) using GoTaq Polymerase
234 G2 (Promega) as described by Promega including: 1X green GoTaq reaction buffer
235 (Promega), 0.2 mM of each dNTP, 0.5 µM of each primer and 1.25 U of GoTaq DNA
236 polymerase (Promega). After a first denaturation step of 5 min at 95°C, thirty-five cycles of
237 three steps were carried out as follows: denaturation for 30 s at 95°C, annealing for 30 s at
238 56°C and extension for 45 s at 72°C. After a final extension for 10 min at 72 °C and a last

239 step at 4 °C, amplified PCR products were checked on a 1% agarose gel and purified
240 directly using Wizard SV Gel and PCR clean-up System (Promega) as recommended by
241 the manufacturer. The two purified amplicons were double-strand sequenced using ITS-
242 85/ITS-750 primers. Species identity of the two monoclonal cultures was confirmed by
243 submitting both sequences to the NCBI non-redundant (nr) database (BLASTn) (Figure
244 S2). Both sequences were deposited in GenBank (accession no. MW187111 for the *P.*
245 *olseni* monoclonal culture and MW187112 for the *P. chesapeaki* monoclonal culture).

246

247 **2.5.2. Production of specific *P. olseni* and *P. chesapeaki* plasmid standards**

248 Plasmid standards are a useful resource for relative quantification of parasite in host
249 tissue. The methodology used to establish the two standards was based on the duplex
250 study between *Perkinsus* and *Haplosporidium* species from Xie *et al.* (2013). ITS
251 sequences were cloned using the pGEM-T easy vector system I (Promega) and
252 transformed into homemade competent *Escherichia coli* XGold following the
253 manufacturer's recommendations. Clones were blue/white screened and numerous
254 clones per library were selected for overnight growth in Lysogeny Broth media (LB) at
255 37°C. Plasmid DNA was purified using the NucleoSpin Plasmid kit (Macherey-Nagel) and
256 quantified using the Qubit™ dsDNA HS assay kit (Invitrogen). Plasmid count was
257 obtained using the following formula: $molecule/\mu l = a / (3\ 665\ bp \times 660\ Da) \times 6.022 \times 10^{23}$
258 where *a* is the DNA plasmid concentration, 3665 bp is the full-length plasmid including
259 the vector (3015 bp) and the amplified fragment (650 bp), 660 Da is the molecular
260 weight of one base pair and 6.022×10^{23} is the Avogadro molecular constant.

261

262 **2.5.3. Design of species-specific primers and TaqMan hydrolysis probes**

263 With their high genetic polymorphism allowing species-level discrimination, ITS regions
264 have been commonly selected as good candidate regions for species-specific primer
265 development (Casas *et al.*, 2002a; b; OIE, 2019b). Primers and probes were designed
266 using Primer3Plus (qPCR settings) (Untergasser *et al.*, 2012) with GenBank-accessed
267 template sequences JQ669642, KX514117, KX514123, LC431768, DQ516714,
268 MG733367, MG733365, KP764683, KX514103, KP764681, FJ481986, and EU293848 for

269 *P. olsenii*, and EU919479, EU919489, EU919501, AY876312, AY876314, EU919465,
270 EU919496, AY876318, AY876316, MF186901, MF186913, and MF186910 for *P.*
271 *chesapeakei*. To optimise the duplex real-time PCR, sets of primers and probes were
272 designed with similar annealing temperatures (T_m) and amplicon lengths (Figure 1;
273 Table 1). Specificities were assessed *in silico* using (1) ARB Software (Ludwig *et al.*,
274 2004) against a multiple sequence alignment of *Perkinsus* ITS1- 5.8S – ITS2 region
275 constructed from sequences available on GenBank (accessed March 2019) (Table S2);
276 (2) Primer-BLAST (accessed March 2019) against the NCBI nonredundant (nr) DNA
277 database (available at <https://www.ncbi.nlm.nih.gov/tools/primer-blast/>) (Table S3);
278 and (3) Blastn submitting probes sequences to the NCBI nr database (available at
279 blast.ncbi.nlm.nih.gov) (Table S4). Secondary structure and dimer formation were
280 checked using the OligoEvaluator (Sigma-Aldrich).

281

282 **2.5.4. Real-time PCR assays development**

283 Real-time PCR assays were performed with the LightCycler 480 Probes Master (Roche)
284 specifically developed for the hydrolysis probes reaction using the LightCycler 480 II
285 (Roche).

286 The specificity of primers and probes were firstly tested using gDNA of the two
287 monoclonal strains of *P. olsenii* and *P. chesapeakei*. Gill gDNA from an uninfected clam was
288 used to confirm the absence of hybridisation with the host matrix. For all conditions, a
289 negative control (pure water) was added to verify the non-contamination of the qPCR
290 mixture and the formation of chimeras. All gDNA concentrations were adjusted to 1 pg
291 using the Qubit dsDNA HS assay kit (Invitrogen).

292 All qPCR assays were performed as recommended by the supplier LightCycler 480
293 Probes Master (Roche). Primers and probes were respectively diluted in pure water at
294 50 μ M and 2 μ M to reach the recommended working solution concentration. The mix
295 LightCycler 480 Probes Master 2X conc. (Roche) contains FastStart Taq DNA
296 Polymerase, reaction buffer, dNTP mix (with dUTP instead of dTTP) and 6.4 mM MgCl₂.
297 The reaction volume for duplex qPCR consisted of 1X LightCycler 480 Probes Master
298 premixed, 0.2 μ M of primer PolsITS2-F, 0.2 μ M of PolsITS2-R, 0.2 μ M of PchesITS2-F, 0.2
299 μ M of PchesITS2-R, 0.5 μ M of PolsITS2-probe (FAM), 0.5 μ M of PchesITS2-probe

300 (LC640), and 5 μ L of DNA sample with adjusted concentration. The reaction volume for
301 simplex qPCR consisted of 1X LightCycler 480 Probes Master premixed, 0.2 μ M of primer
302 P_{olsITS2-F} or P_{chesITS2-F}, 0.2 μ M of P_{olsITS2-R} or P_{chesITS2-R}, 0.5 μ M of P_{olsITS2-}
303 probe or P_{chesITS2-probe}, and 5 μ L of DNA sample with adjusted concentration. The
304 thermal cycling conditions were as follows: 5 min of pre-incubation at 95 °C followed by
305 45 cycles of amplification containing 10 s of denaturation at 95°C and 20 s of annealing
306 at 55°C. At the 72°C extension step, for each cycle a single fluorescence acquisition was
307 recorded for the following filter combination: FAM (465-510), VIC/HEW/Yellow555
308 (533-580) and Cy5/Cy5.5 (618-660). The PCR assay was finally terminated by cooling
309 for 2 min at 40°C. In each qPCR run, samples were run in triplicate and two negative
310 controls containing non-infected Manila clam gDNA and pure molecular grade water
311 were included. Triplicates were averaged for each sample. If one or two values of a
312 triplicate were anomalous, the sample was reprocessed to discard a potential
313 manipulation error.

314

315 **2.5.5. Repeatability of the duplex qPCR method**

316 The variation of the duplex qPCR method was evaluated depending on the repeatability
317 of the 10-fold dilution plasmid standards of *P. olseni* and *P. chesapeaki* from different
318 qPCR runs. The coefficient of variation (CV) was calculated as follows: $CV = \frac{sd}{\bar{x}} \times 100\%$
319 (sd: standard-deviation and \bar{x} : mean related to one plasmid dilution) for each dilution
320 (2.5×10^1 to 2.5×10^6 total copies) of the reference standards. For each dilution, the means
321 of Ct values and standard deviations were calculated from six different qPCR runs. The
322 coefficients of variation were then calculated for all plasmid concentrations.

323

324 **2.6. Inhibitory effect of host tissue on the qPCR assay**

325 First, standard curves (supplemented with water) were crossed and determined by
326 duplex qPCR assay to establish reference values of non-inhibited reactions for both
327 species. The sensitivity of the duplex qPCR was estimated on plasmid-inserted ITS1-
328 5.8S-ITS2 of *P. olseni* and *P. chesapeaki* with 10-fold serial dilutions from 2.5×10^1 to
329 2.5×10^6 total copies in triplicates. Sensitivity is represented by two parameters: 1) the

330 efficiency (E), which is the evaluation of the fraction of target molecules that are copied
331 in one PCR cycle, where 100% represents an optimal doubling amount of DNA; and 2)
332 the limit of detection (LOD), which is the lowest plasmid concentration giving positive
333 and homogeneous Ct (Cycle threshold) values. Standard curves were represented by
334 plotting the logarithm of the plasmid copy number against the corresponding measured
335 Ct value. Thus, the qPCR efficiency (%) was calculated, depending on the slope of each
336 curve of serial diluted target, as follows: $E = (10^{-1/\text{slope}} - 1) \times 100\%$. The detection limit
337 (number of total copies) was determined as the lowest concentration of plasmids within
338 the linear range showing significant and homogeneous amplification signal in triplicate
339 using the LightCycler 480 v. 1.1.1.62 software (Roche).

340 Then, qPCR assays were carried out to determine the effects of the host gDNA organ type
341 (i.e. gill, digestive gland, adductor muscle, foot, mantle and the remaining tissue) on the
342 sensitivity of the qPCR duplex reaction. Based on RFTM and qPCR assay results, three
343 *Perkinsus*-free clams were selected to determine the possible inhibitory effect for each
344 organ type. To assess a global trend of organ influence, the mean Ct value and the
345 standard errors were calculated from the three *Perkinsus*-free individuals for each
346 concentration. Parameters of sensitivity for the two assays were determined in duplex
347 reaction on crossed 10-fold serial dilutions of *P. olseni* and *P. chesapeaki* plasmids DNA
348 (2.5×10^1 to 2.5×10^6 total copies) supplemented with a dilution (2, 5, 10, and 20 $\text{ng} \cdot \mu\text{L}^{-1}$)
349 of host gDNA organ. In each qPCR assay, inhibitor-free standard curves (without host
350 gDNA extract) were added and Ct values were measured.

351 Standard dilution curves supplemented with extracted of organ gDNA were represented
352 by plotting the logarithm of the plasmids copy number against the corresponding
353 measured Ct value. Standard curves (plasmids only) determined above were plotted as
354 an organ-free reference for each duplex qPCR to compare possible inhibition effect of
355 each organ on the value of efficiency (%). The qPCR efficiency of the reaction for each
356 condition was calculated from each standard curve as described above. The detection
357 limit (number of total copies) was determined as the lowest concentration of plasmids
358 within the linear range showing significant and homogeneous amplification signal in
359 triplicate using LightCycler 480 v. 1.1.1.62 software.

360

2.7. Comparison of the duplex qPCR and the RFTM method on gill tissue

Comparison of RFTM and qPCR methodologies on gill tissue (the most currently targeted tissue for perkinsosis detection) is essential to validate the molecular assay developed in this study. To compare perkinsosis results obtained with the standard RFTM method and the duplex real-time PCR method, all 50 gill DNA samples were tested by duplex qPCR. To ensure a reliable comparison between infected individuals, the concentrations of all gill DNA samples were adjusted to 20 ng.µL⁻¹ as determined above. The qPCR was then run in triplicate using the same parameters as above. The 10-fold dilution plasmid standards for *P. olseni* and *P. chesapeakei* were added to the run to determine copy concentrations in gill tissue. The mean copy number per sample was automatically calculated by the LightCycler 480 v. 1.1.1.62 software. The intensity of infection was calculated from the number of copies detected divided by the wet weight of the corresponding gill for each species of parasite.

2.8. Statistical analysis

The inhibitory effect of organ gDNA extracts at several concentrations (20, 10, 5, 2 ng.µL⁻¹) were compared to determine which concentrations represented the best dilution to optimise *Perkinsus* detection in tissue. Each linear curve was compared to the standard 10-fold plasmids dilution by a one-way analysis of covariance (ANCOVA). The majority of variables tested for each inhibitory condition fulfilled assumptions for application of ANCOVA. Plasmid concentrations were log-transformed. A regression model was fitted (Rainbow test, p-value > 0.05). Residuals were independent (Durbin-Watson test, p-value > 0.05) and normally distributed (Shapiro-Wilk test, p-value > 0.05). Homogeneity of variances was verified (Bartlett test, p-value > 0.05). The ANCOVA was used to evaluate the effect of organ on Ct values depending on organ concentration (covariate). Curves showing no significant differences from the standard 10-fold plasmids dilution were selected as good candidates for *Perkinsus* detection. Absence of difference from the standard demonstrated a reaction non-inhibited by host DNA extract. If several curves showed no significant difference, the highest concentration of organ DNA was adopted to optimise *Perkinsus* detection.

391 The agreement between the duplex qPCR assay and the RFTM assay to measure
392 infection intensity was evaluated by descriptive parameters and statistical analysis.
393 *Perkinsus* prevalences (proportion of infected individuals to the total number of hosts
394 sampled, %) were determined for both methods and the species was determined when
395 possible. Two parameters, the concordance and the discordance, were adapted for this
396 study from Langton *et al.* (2002) and calculated. The concordance, calculated by
397 counting pairs of positive samples and pairs of negative samples, is the percentage of
398 chance that an identical sample analysed by two different methodologies will have the
399 same result. The discordance, calculated by counting the unpaired samples (i.e. positive
400 by RFTM and negative by qPCR assay, and vice versa), is the percentage chance that an
401 identical sample analysed by two different methodologies will have the different result.
402 The relationship between both methods was tested using a linear model and the
403 Spearman correlation coefficient on infection intensities from qPCR and RFTM positive
404 individuals.

405 Finally, the mean infection intensities determined by both methods were compared to
406 verify their congruence. The infection intensities related to plasmid quantifications were
407 evaluated in number of cells per gram of wet gill with the relationship established
408 between the qPCR assay and the RFTM assay ($y=0.60x+4.36$; y : log of qPCR-infection
409 intensity in number of copies.g of wet gill⁻¹; x : log of RFTM-infection intensity in number
410 of cells.g of wet gill⁻¹).

411

412 **3. Results**

413

414 **3.1. Specificity of the PCR assay**

415

416 Primer and probe design is a crucial step for an accurately duplexing real-time PCR
417 assay. *In silico* tests demonstrated that primers and probes were dissimilar in sequence
418 to closely related *Perkinsus* species sequences and other important parasitic or
419 heterotrophic protist families described in clam populations and in surrounding
420 environments (Table S2, S3, S4).

421 Molecular tests were conducted by comparing the same amount (1 pg) of *P. olseni* and *P.*
422 *chesapeakei* gDNA extracted from monoclonal cultures. For the *P. olseni* primers
423 (PolsITS2_F/PolsITS2_R) and probe (PolsITS2_probe) set, amplification (Ct: 26.4 ± 0.07)
424 was detected using *P. olseni* gDNA as a template with the filter FAM (465-510
425 wavelengths) corresponding dye excitation wavelength coupled with *P. olseni* probe
426 (Figure 2). As expected, no amplification was detected for all wavelengths with *P.*
427 *chesapeakei* gDNA, host gDNA or pure water as template.

428 The *P. chesapeakei* primers (PchesITS2_F/PchesITS2_R) and probe (PchesITS2_probe) set
429 amplified (Ct: 26.7 ± 0.09) only *P. chesapeakei* gDNA with the suitable filter LC640 (618-
430 660 wavelengths), and no amplification was detected for other wavelengths or other
431 templates, *P. olseni* gDNA, host gDNA and pure water (Figure 2). These results
432 demonstrate that the qPCR primers and probes sets are specific to the targeted gDNA
433 without any cross amplification.

434

435 3.2. Standards PCR sensitivity and repeatability

436

437 Given the unknown number of ribosomal operons in parasite genomes and the ploidy
438 and nuclear count of each life stage, plasmids are useful as a reproducible and stable
439 standard for qPCR assays (Dhanasekaran *et al.*, 2010). The ITS sequence of each parasite
440 culture was isolated via plasmid purification from cloned and transformed competent
441 bacteria. Two standard curves (*P. olseni*: $y = -3.33x + 39.49$; *P. chesapeakei*: $y = -3.38x +$
442 40.29 ; Figure 3) were generated from 10-fold serial dilutions from 2.5×10^1 to 2.5×10^6
443 copies of ITS rDNA plasmid. Ct values of both standard curves showed strong linear
444 correlations with the targeted template (*P. olseni*: $R^2 = 0.95$; *P. chesapeakei*: $R^2 = 0.95$;
445 Figure 3). The limit of detection was determined to be 25 copies of the target DNA in a
446 10- μ L reaction volume; below this number of plasmid copies (2.5 copies; data not
447 shown), triplicates displayed non-replicable Ct values. DNA amplification was detected
448 within the range of 2.5×10^1 to 2.5×10^6 plasmids with Ct values ranging from 34.9 ± 1.6
449 to 18.8 ± 1.5 and to 35.1 ± 1.6 to 18.4 ± 1.5 for *P. olseni* and *P. chesapeakei* respectively.
450 The efficiency of each set of primers is evaluated from standards at 99.8% for *P. olseni*
451 and 97.8% for *P. chesapeakei* (Figure 3). The theoretical maximum of 1.0 (or 100%)
452 indicates that the amount of product doubles with each cycle (Bustin *et al.*, 2009).

453 The coefficient of variation (CV) for the duplex qPCR method was estimated for *P. olseni*
454 standard between 3 to 8% (Table 2).

455

456 **3.3. Inhibitory effects of host tissue gDNA extract on the duplex qPCR assays**

457 Organ gDNA extract may have inhibitory effects on the efficiency of the qPCR
458 amplification. To test this organ-dependent qPCR effect, the sensitivity and the
459 inhibition of the duplex qPCR assay were evaluated according to the type of organ (gill,
460 digestive gland, adductor muscle, foot, mantle and remaining tissue) at different
461 concentrations of gDNA (2, 5, 10, 20 $\mu\text{g}\cdot\mu\text{L}^{-1}$). Ct values varied from *P. olseni* and *P.*
462 *chesapeaki* standards depending on organ type and gDNA concentration used for the
463 amplification (Figure 4). Results of ANCOVA and efficiencies are synthesised in Table S5.
464 Efficiencies (E) between 90% and 110% are tolerated for a complex host matrix even if
465 slight over- and under-estimation can happen.

466

467 **3.3.1. Effect of organ gDNA extracts on *P. olseni*-plasmid detection**

468 *P. olseni*-standards containing only plasmids represented the positive control with an
469 amplification of *P. olseni* gDNA in absence of inhibitory effects (Figure 3). For gill and
470 digestive gland, the four concentrations did not influence the linear 10-fold dilution
471 curves (ANCOVA, p-value >0.05) (Figure 4A). With no difference observed from the
472 standard curve, the maximum concentration is 20 $\text{ng}\cdot\mu\text{L}^{-1}$ for gDNA of both gills
473 (efficiency (E) = 100.3%) and digestive gland (E = 100.4%). For the adductor muscle,
474 only the amplification curve corresponding to 20 $\text{ng}\cdot\mu\text{L}^{-1}$ showed a significant difference
475 from the *P. olseni* standard (ANCOVA, F=5.53, p-value < 0.05). It had a high efficiency of
476 115.4 %. Maximum concentrations showing no difference from the standard were the 10
477 $\text{ng}\cdot\mu\text{L}^{-1}$ and 5 $\text{ng}\cdot\mu\text{L}^{-1}$ curves (ANCOVA, p-value >0.05). The 5 $\text{ng}\cdot\mu\text{L}^{-1}$ curve was preferred
478 for its optimal efficiency of 98.7%. For foot, the amplification curves corresponding to 10
479 $\text{ng}\cdot\mu\text{L}^{-1}$ and 20 $\text{ng}\cdot\mu\text{L}^{-1}$ showed significant differences from the *P. olseni* standard
480 (ANCOVA, $F_{10\text{ng}/\mu\text{L}}=8.4$, p-value $_{10\text{ng}/\mu\text{L}} < 0.01$; $F_{20\text{ng}/\mu\text{L}}=17.6$, p-value $_{20\text{ng}/\mu\text{L}} < 0.001$). The
481 maximum concentration with no difference from the standard was the 5 $\text{ng}\cdot\mu\text{L}^{-1}$ curve (E
482 = 92.8% ; ANCOVA, p-value >0.05). For mantle, the 2 $\text{ng}\cdot\mu\text{L}^{-1}$ was the maximum
483 concentration that did not alter the linear 10-fold dilution curve (E = 92% ; ANCOVA, p-

484 value >0.05). Even if the amplification curves for 5 ng.μL⁻¹ and 20 ng.μL⁻¹ showed non-
485 significant differences from the standard, their shifts are out of the error range, which
486 highlights an important variability for these concentrations (Figure 4A). For the
487 remaining tissue, 2 ng.μL⁻¹ was the maximum concentration of gDNA that did not alter
488 the linear 10-fold dilution curve (E = 105.6% ; ANCOVA, p-value >0.05). Other
489 concentrations showed significant differences or efficiencies too high (e.g. the 10 ng.μL⁻¹
490 curve: E = 121.7%) to be selected.

491

492 **3.3.2. Effect of organ gDNA extracts on *P. chesapeaki*-plasmids detection**

493 Same trends are observed for *P. chesapeaki* where standard containing only plasmids
494 represented the positive control without any inhibitory effects (Figure 3). For gill and
495 digestive gland, the addition of gDNA extract did not influence the linear 10-fold dilution
496 curves at any of the tested concentrations (ANCOVA, p-value >0.05) (Figure 4B). With no
497 difference observed from the standard curve, the maximum concentration was 20 ng.μL⁻¹
498 for gDNA of both gills (E = 98.3%) and digestive gland (E = 97.2%). For the adductor
499 muscle, the curve corresponding to 10 ng.μL⁻¹ showed a significant difference from the
500 standard (ANCOVA, $F_{10\text{ng}/\mu\text{L}}=5.5$, p-value < 0.05). The maximum concentration showing
501 no difference from the standard was the 5 ng.μL⁻¹ curve (E = 96.3% ; ANCOVA, p-value
502 >0.05). For foot, the gDNA concentrations of 10 ng.μL⁻¹ and 20 ng.μL⁻¹ showed significant
503 differences from the *P. chesapeaki* standard (ANCOVA, $F_{10\text{ng}/\mu\text{L}}= 26.6$, p-value_{10ng/μL}
504 <0.001; $F_{20\text{ng}/\mu\text{L}}= 16.1$, p-value_{20ng/μL} <0.001). The maximum concentration of foot gDNA
505 extract with no difference from the standard was the 5 ng.μL⁻¹ curve (E = 89.3%;
506 ANCOVA, p-value >0.05) even if the efficiency indicated a slight underestimation of the
507 target. For mantle, 2 ng.μL⁻¹ was the maximum concentration that did not alter the linear
508 10-fold dilution curve (E = 92.1%, ANCOVA, p-value >0.05). The curve corresponding to
509 5 ng.μL⁻¹ showed a non-significant difference from the standard but was discarded due
510 to a lower concentration threshold for *P. olseni* (2 ng.μL⁻¹). The host tissue gDNA
511 concentration of 2 ng.μL⁻¹ was the safest trade-off showing no difference from the
512 standard. For the remaining tissue, the 2 ng.μL⁻¹ was the maximum concentration of
513 gDNA that did not alter the linear 10-fold dilution curve (E = 95.7%; ANCOVA, p-value
514 >0.05).

515

516 3.4. Comparison of two quantitative methods: RFTM and qPCR duplex on gill 517 tissue samples

518

519 To evaluate the effectiveness of the qPCR assay for detecting and quantifying *P. olseni*
520 and *P. chesapeaki* levels in clam gill, the copy number estimated with this method for
521 each prevalent species was determined and compared with the RFTM infection
522 intensities.

523 Based on the previous results described above, only Ct values within the standard range
524 of 2.5×10^1 to 2.5×10^6 total copies were considered positive. Therefore, all values below
525 this range were considered as unquantifiable. No samples were quantified above
526 2.5×10^6 total copies. The total prevalence of *Perkinsus* estimated by RFTM assay and
527 qPCR assay was 74%, representing a total of 37 infected clams over the 50 clams tested
528 (Table 3). Prevalence of *P. olseni* single infections represented 68% (34 clams) of
529 sampled individuals whereas co-infection represented only 6% (3 clams). Among the co-
530 infected hosts (n=3), the *Perkinsus* spp. mean infection intensity was $1.37 \times 10^4 \pm$
531 2.14×10^4 cells. g⁻¹ of wet tissue. Based on paired and unpaired prevalences from both
532 RFTM and qPCR assays, the concordance was estimated at 88% and the discordance at
533 12% (Table 4). The three discordant individuals, positive by RFTM assay and negative
534 with qPCR assay, showed very light infection intensities ranging from 8.1 cells.g⁻¹ of wet
535 tissue to 6.0×10^2 cells.g⁻¹ of wet tissue.

536

537 To determine the relationship between both quantitative methods, only positive clams
538 by RFTM and qPCR were compared (Figure 5). A linear regression was determined for
539 the qPCR-infection intensity and the RFTM-infection intensity relationship
540 ($y=0.60x+4.36$, adjusted-R²=0.61, n=34). A significant Pearson's coefficient was obtained
541 for the qPCR-infection intensities and the RFTM-infection intensities (r=0.79, p-
542 value<0.001) showing a positive correlation. The infection intensity (in cells.g⁻¹ of wet
543 tissue) for each individual was evaluated from the qPCR assay following the relationship
544 described before ($y=0.60x+4.36$; Figure 5). A discrepancy from the linear regression line
545 was observed for low infection values (below 100 cells.g⁻¹ of wet gill). To optimise
546 parasite detection, negative individuals and mismatched individuals were discarded.
547 Consequently, the intercept of this linear relationship is not equal to zero which

548 introduces an overestimation of infection intensity. The mean infection intensity
549 estimated by qPCR assay was $3.35 \times 10^5 \pm 8.55 \times 10^5$ cell. g⁻¹ of wet tissue. Separately,
550 mean infection intensity for *P. olseni* was estimated at $1.37 \times 10^4 \pm 2.14 \times 10^4$ cells.g⁻¹ of
551 wet tissue and for *P. chesapeakei* at $2.50 \times 10^1 \pm 2.69 \times 10^1$ cells.g⁻¹ of wet tissue. The mean
552 proportion of *P. olseni* was $9\% \pm 5\%$.

553

554

555 **4. Discussion**

556

557 **4.1. The RFTM assay lacks specificity**

558 Almeida *et al.* (1999) suggested that planktonic organisms like dinoflagellates could
559 react positively in RFTM assays, highlighting a lack of genus-specificity when used on
560 environmental samples by [inadequately expert diagnosticians](#). This standard
561 methodology also lacks species specificity, hypnospores showing no distinctive
562 morphological traits, and furthermore does not detect all *Perkinsus* parasites: *P. qugwadi*
563 does not form hypnospores in RFTM and thus may not be detected by the assay (Itoh *et*
564 *al.*, 2013). Using only this methodology allows estimation of the prevalence and
565 intensities of “generic” *Perkinsus* infection, acceptable when only a single species is
566 present, but it will miss cryptic co-infections, as noted for *P. marinus* and *P. chesapeakei* in
567 Chesapeake Bay (Reece *et al.*, 2008).

568 Using the RFTM methodology, we observed 74% prevalence with a strong infection
569 intensity of $9.04 \times 10^4 \pm 2.24 \times 10^5$ cells.g⁻¹ of wet tissue, is consistent with the results
570 obtained by Dang *et al.* (2010) from Arcachon Bay in November 2006 and 2007 where
571 prevalences were 75% and 70% and infection intensities of 1.58×10^5 and 7.94×10^4
572 cells.g⁻¹ of wet tissue respectively. However, the diversity of *Perkinsus* species occurring
573 in Arcachon Bay is yet not resolved. From a previous sampling campaign carried out in
574 October 2017 in Arcachon Bay (data not shown), *Perkinsus* culture cell lines were
575 established from clam gill samples. The genetic diversity in the ITS1-5S-ITS2 rDNA
576 region revealed that 17 cultures (of n = 22) were 100% similar in sequence to *P. olseni*
577 across 627 bp, while 5 cultures were 97-100% similar to *P. chesapeakei* across 639 bp. All
578 these results are congruent with previous studies showing co-occurrence of these two
579 *Perkinsus* species in European coastal environments (Arzul *et al.*, 2012; Ramilo *et al.*,
580 2016). Hence, the *in situ* occurrence of these cryptic infections in the Arcachon Bay has

581 made necessary the development of a non-culture based method like the duplex qPCR to
582 distinguish between two parasites, *P. olseni* and *P. chesapeaki*, in Manila clam tissue
583 samples.

584

585

586 **4.2. The real-time PCR improved our conception of *in situ* infection**

587 Real-time PCR methodology has largely proven to be successful for the diagnose of *in*
588 *situ* infection by protists, viruses or bacteria (Hardegen *et al.*, 2010; Kuhar *et al.*, 2013;
589 Duffy *et al.*, 2013). In context of emerging diseases in aquaculture, it brings a new
590 perspective on species occurrence and intensity of infection (Gauthier *et al.*, 2006; Ulrich
591 *et al.*, 2007; Umeda and Yoshinaga, 2012; Cui *et al.*, 2018). Detection of perkinsosis has
592 been accomplished using two types of real-time PCR chemistry, SYBR Green (Audemard
593 *et al.*, 2004; Ulrich *et al.*, 2007) and TaqMan (Gauthier *et al.*, 2006; Marquis *et al.*, 2020).
594 The TaqMan-based real-time PCR provides a multiplexing ability which allows multiple
595 detection in one run while reducing technical bias (Elnifro *et al.*, 2000). In the duplex
596 qPCR specificity experiments performed in this study, Ct values are similar for an
597 amount of 1 pg of *P. olseni* and *P. chesapeaki* gDNA when using corresponding primers
598 and probes in their respective wavelengths (*P. olseni*-Ct value: 26.4 ± 0.07 ; *P. chesapeaki*-
599 Ct value: 26.7 ± 0.09). Hence, our results support the hypothesis that *P. olseni* and *P.*
600 *chesapeaki* might possess very similar numbers of ITS2 copies in their genomes allowing
601 an easy comparison of infection intensity between both parasitic species.

602 In 2020, Marquis *et al.* highlighted the dynamics of *P. marinus*, *P. chesapeaki* and
603 *Haplosporidium nelsoni* in oysters from the Gulf of Maine during summer-fall 2016 and
604 2017 showing the rising interest of this technique in the management of marine disease
605 (Marquis *et al.*, 2020). Development of a molecular multiplexing approach may be
606 particularly useful in environments where multi-species infection seems to be the rule
607 (Bass *et al.*, 2019). The duplex qPCR method elaborated in this study demonstrates low
608 inter-plate qPCR variation (CV% from 5% to 8 %, Table 2), a testament to its
609 repeatability. Thus, we confirm the utility of TaqMan methodology for the relative
610 quantification of *P. olseni* and *P. chesapeaki* based on reliable and repeatable plasmid-

611 standards (from 2.5×10^1 to 2.5×10^6 total copies) and for perkinsosis in Europe generally,
612 which may sometimes involve cryptic dual infections.

613

614 **4.3. PCR inhibitors contained in biological tissue are a very common issue** 615 **linked to qPCR assays**

616 Inhibition effects are recognized issues for parasite detection within host samples
617 (Audemard *et al.*, 2004, 2006). Organic and inorganic compounds present in the host
618 matrix and extracted with gDNA may compromise the efficiency of DNA polymerases
619 and ultimately produce false negative results or erroneous Ct values (De Faveri *et al.*,
620 2009). By producing standard curves supplemented with different concentrations of
621 extract of organs gDNA, we showed here that PCR inhibitors are present in some clam
622 organs but can be resolved by adjusting template gDNA concentrations.

623 In this study, quantification of plasmid standards (a useful and accurate proxy for
624 *Perkinsus*) was tested with six different concentrations of gDNA organs (gills, digestive
625 gland, foot, adductor muscle, mantle and the remaining tissue). For both *Perkinsus*
626 species, gill and digestive gland gDNA extracts did not contain inhibitory compounds in
627 the range of the qPCR detection as already described for gill tissue by Umeda and
628 Yoshinaga (2012). Thus, for these two types of tissue, the gDNA concentration may
629 easily reach $20 \text{ ng} \cdot \mu\text{L}^{-1}$ within the qPCR framework described above to optimise
630 *Perkinsus* detection and avoid qPCR saturation. Conversely, adductor muscle and the
631 foot on one hand and mantle and remaining tissues on the other showed optimal
632 amplification at host gDNA concentrations of $5 \text{ ng} \cdot \mu\text{L}^{-1}$ and $2 \text{ ng} \cdot \mu\text{L}^{-1}$ respectively. These
633 results are surprising because unlike in clams, mantle and the rectum tissue from
634 oysters had no inhibitory effects on qPCR reactions (De Faveri *et al.*, 2009). A lower load
635 of organ gDNA, e.g. $2 \text{ ng} \cdot \mu\text{L}^{-1}$, decreases the detection limit of the parasite compared to a
636 higher load. Thus, for organs like mantle or remaining tissues, the prevalence of
637 *Perkinsus* parasite may be underestimated in cases of low infection intensity. The
638 thresholds mentioned in this study are basic recommendations for duplex TaqMan-
639 based real-time PCR applied to further studies on the parasite dynamics in the Manila
640 clam. These values are specific to the Manila clam and should be adjusted for each
641 biological model and targeted organ. In spite of inter-individual variability between the
642 three non-infected reference Manila clams used for the inhibitory test, a very clear
643 inhibition trend related to the type of clam organ is observed. This kind of observation

644 testifies to the appropriateness of gill for routine diagnostic for molecular methods
645 including PCR and qPCR, as this organ is not inhibitory and a reasonable target tissue to
646 detect *Perkinsus* infection.

647

648 **4.4. Correlation between RFTM methodology and molecular tools: toward a** 649 **consensus method for the *Perkinsus* diagnosis**

650 This study highlights a significant linear relationship of the duplex qPCR method and the
651 RFTM method on gill tissue samples. Even if the Spearman's coefficient is not as high as
652 expected (Ríos *et al.*, 2020), two hypothesis can explain the difference between both
653 measures. First, there is a fundamental difference between both methodologies in terms
654 of analytical effort. Indeed, a small fraction of total gDNA amount is analysed for the
655 molecular method whereas the RFTM allows counting the entire gill in case of low
656 infection intensity. Secondly, in this study, we decided to exploit each gill of an
657 individual separately (see Material & Methods) instead of shredding both parts together
658 and losing some more fragile parasitic cells. The asymmetrical infection of *Perkinsus* sp.
659 of clam gills may induce some mismatches connecting the two methods. This divergence
660 is mostly observed at the lower limits of the qPCR standards, from 2.5×10^1 to 2.5×10^2
661 total copies. For other standard-points (i.e. from 2.5×10^2 to 2.5×10^6 total copies), the
662 higher infection intensities enable a more homogeneous distribution of parasites in the
663 gill and therefore better qPCR detection. Most of the positive individuals (32 of 34
664 paired-positive Manila clams) were localised in the range of 2.5×10^2 to 2.5×10^6 total
665 copies leading to good correlation between RFTM and qPCR assay quantification.

666 In this study, there was no difference in prevalence (74% with 88% of concordance).
667 However, we observed that the mean infection intensity for the RFTM method (9.04×10^4
668 $\pm 2.24 \times 10^5$ cells. g⁻¹ of wet tissue) seemed lower than the qPCR assay ($3.35 \times 10^5 \pm$
669 8.55×10^5 cell. g⁻¹ of wet tissue). These values should be interpreted with caution because
670 of the small number of individuals sampled (n=50). Such difference could be explained
671 by several hypothetical biases. First, the two methods would interact with parasite cell
672 nuclear count differently, the RFTM assay registering all *Perkinsus* hypnospores present
673 as individual cells, but the qPCR on the other hand registering multinucleate schizonts as
674 greater template DNA abundance equating, inaccurately, to higher numbers of individual
675 parasite cells. The presence of multinucleate schizonts would thus have the effect of

676 inflating parasite intensity as perceived by qPCR. Second, and to the contrary, an
677 incomplete transformation of the intra-host population of trophozoites and schizonts
678 into hypnospores could conceivably lead to RFTM results underestimating the overall
679 infection intensity. This underestimation might be accentuated for the lowest infection
680 intensities (e.g. for 8.1 to 6.0×10^2 cells.g⁻¹ of wet tissue in this study). The physiological
681 status of the parasite and incomplete hypnospore formation could have a much greater
682 impact on the estimation of low infection intensities than intensities comprising
683 thousands of cells per gram of tissue. In addition, the infection intensities of the duplex
684 qPCR are indirectly estimated by a mathematical relationship ($y=0.6041x+4.3459$;
685 adjusted-R² = 0.61) relying on the RFTM counting method. Moreover, this linear
686 equation has a positive value of intercept which impacts strongly lowest values of
687 infection.

688 The molecular method, in other words, measures a total amount of DNA copies
689 regardless of the physiological stage of *Perkinsus* cells while the traditional RFTM
690 method allows the counting of trophozoites that are able to transform into hypnospores.
691 Given their respective biases, it is not surprising that qPCR infection intensity values
692 appear to be higher than those of the RFTM assay. The duplex qPCR method nonetheless
693 is a useful alternative to RFTM for application in many situations.

694

695 **4.5. Application of the concept: *in situ* co-infection**

696 The relationship between detection methods allowed us to evaluate the prevalence and
697 intensity of infection of both parasites *P. olseni* and *P. chesapeaki* in a same host gill
698 tissue sample. At the Lanton station, co-infection was observed at very low frequency
699 (6%, n=3/50 individuals sampled). *P. olseni* largely dominates the cases of single
700 infection and remains preponderant in co-infections. Conversely, *P. chesapeaki* is less
701 prevalent and present at much lower intensities. We demonstrated that *P. olseni* invades
702 the gill more efficiently, with 95% of occupation compared to *P. chesapeaki*. Indeed, *P.*
703 *chesapeaki* represents only 5% of the parasitic load in the co-infected clams. Initial
704 evidence leads to us believe that the distribution between *P. olseni* and *P. chesapeaki*
705 may not be homogeneous within clam organs. Arzul *et al.* (2012) described in *R.*
706 *decussatus*, via *in situ* hybridisation methodology, that *P. olseni* is more widespread and

707 abundant in host tissues compared to *P. chesapeaki*. The distribution of *P. olsenii* shows a
708 differential organ propagation depending on the infection stage (Wang *et al.*, 2018).
709 Globally, it is assumed that gill infection is representative of the distribution of the
710 parasite through the clam or oyster body (Yarnall *et al.* 2000) but in case of multiple
711 infections the parasite tropism could be different depending on their interactions and
712 their spatial and temporal dynamics (Cui *et al.*, 2018). The development of a duplex
713 qPCR method allowed easier detection and quantification of the co-infection
714 phenomenon and determination of the abundance of each parasite in the infected host.
715 It is critical to consider the whole-body compartment in a host to reach the most
716 accurate diagnostic of perkinsosis caused by *P. olsenii* and *P. chesapeaki*.

717

718

719 **5. Conclusion**

720 When *P. olsenii* and *P. chesapeaki* are detected in a same Manila clam population, a
721 multiplexing qPCR approach is more appropriate even if quantification can be
722 overestimated. RFTM may, conceivably, underestimate results for infection intensity of
723 *Perkinsus*, and we recognize that it is not informative in species-level discrimination
724 when multiple *Perkinsus* species are present. While the standard RFTM culture method
725 and the molecular method are generally equivalent approaches in profiling perkinsosis
726 generically, the specific ability of the qPCR to resolve one *Perkinsus* species or the other
727 will make its use advantageous where species discrimination is necessary. The duplex
728 TaqMan real-time PCR assay is a very sensitive, reproducible and specific method to
729 investigate the *in situ* diversity, distribution and abundance of *Perkinsus* spp. in case of
730 multiple-occurrence. Development of this tool could bring an instantaneous screenshot
731 of the disease state and the dynamics of *Perkinsus* spp. interaction. The localisation and
732 the detection of both parasites are a major challenge in the management of potential
733 valuable hosts living in sympatry. The coupling of both methods is a powerful approach
734 to fully understand perkinsosis dynamics and prevent the spread of these parasites in
735 new hosts and environments.

736

737 **Acknowledgements**

738 SI was funded by a French doctoral research grant from Ecole Doctorale des Sciences de
739 la Mer et du Littoral (EDSML) and Région Bretagne. This work was supported by the
740 ANR project ACHN 2016 PARASED (ANR-16_ACHN_0003) and by the French National
741 program EC2CO (Ecosphère Continentale et côtière) project THRAUSTO (N°13046). The
742 funders had no role in study design, data collection and analysis, decision to publish, or
743 preparation of the manuscript. Samples were performed with Planula 4 vessel (CNRS-
744 INSU, Flotte Océanographique Française).

745 **References**

746 **Allam, B., Paillard, C. and Ford, S. E.** (2002). Pathogenicity of *Vibrio tapetis*, the
747 aetiological agent of brown ring disease in clams. *Diseases of aquatic organisms*
748 **48**, 221–231. doi: 10.3354/dao048221.

749
750 **Almeida, M., Berthe, F., Thébault, A. and Dinis, M. T.** (1999). Whole clam culture as a
751 quantitative diagnostic procedure of *Perkinsus atlanticus* (Apicomplexa,
752 Perkinsea) in clams *Ruditapes decussatus*. *Aquaculture* **177**, 325–332.
753 doi:10.1016/S0044-8486(99)00095.

754
755 **Andrews, J. D.** (1996). History of *Perkinsus marinus*, a pathogen of oysters in
756 Chesapeake bay 1950-1984. *Journal of Shellfish Research* **15**, 13–16.

757
758 **Arzul, I., Chollet, B., Michel, J., Robert, M., Garcia, C., Joly, J.-P., François, C. and**
759 **Miossec, L.** (2012). One *Perkinsus* species may hide another: characterization of
760 *Perkinsus* species present in clam production areas of France. *Parasitology* **139**,
761 1757–1771. doi: 10.1017/S0031182012001047.

762
763 **Audemard, C., Reece, K. S. and Burreson, E. M.** (2004). Real-time PCR for detection
764 and quantification of the protistan parasite *Perkinsus marinus* in environmental
765 waters. *Applied and Environmental Microbiology* **70**, 6611–6618. doi:
766 10.1128/AEM.70.11.6611-6618.2004.

767
768 **Audemard, C., Calvo, L. R., Paynter, K. T., Reece, K. S. and Burreson, E. M.** (2006).
769 Real-time PCR investigation of parasite ecology: *in situ* determination of oyster
770 parasite *Perkinsus marinus* transmission dynamics in lower Chesapeake Bay.
771 *Parasitology* **132**, 827–842.

772
773 **Audemard, C., Carnegie, R. and Burreson, E.** (2008). Shellfish tissues evaluated for
774 *Perkinsus* spp. using the Ray's fluid thioglycollate medium culture assay can be

775 used for downstream molecular assays. *Diseases of Aquatic Organisms* **80**, 235–
776 239. doi: 10.3354/dao01944.
777

778 **Azevedo, C.** (1989). Fine structure of *Perkinsus atlanticus* n. sp. (Apicomplexa,
779 Perkinsea) parasite of the clam *Ruditapes decussatus* from Portugal. *The Journal of*
780 *Parasitology* **75**, 627. doi: 10.2307/3282915.
781

782 **Balseiro, P., Montes, J., Conchas, R., Novoa, B. and Figueras, A.** (2010). Comparison of
783 diagnostic techniques to detect the clam pathogen *Perkinsus olseni*. *Diseases of*
784 *Aquatic Organisms* **90**, 143–151. doi: 10.3354/dao02194.
785

786 **Bass, D., Stentiford, G. D., Wang, H.-C., Koskella, B. and Tyler, C. R.** (2019). The
787 pathobiome in animal and plant diseases. *Trends in Ecology & Evolution* **34**, 996–
788 1008. doi: 10.1016/j.tree.2019.07.012.
789

790 **Batista, F. M., Arzul, I., Pepin, J.-F., Ruano, F., Friedman, C. S., Boudry, P. and**
791 **Renault, T.** (2007). Detection of ostreid herpesvirus 1 DNA by PCR in bivalve
792 molluscs: A critical review. *Journal of Virological Methods* **139**, 1–11. doi:
793 10.1016/j.jviromet.2006.09.005.
794

795 **Bertignac, M., Auby, I., Sauriau, P.-G., De Montaudouin, X., Foucard, J. and Martin, S.**
796 (2001). Evaluation du stock de palourdes du bassin d'Arcachon, Ifremer Report
797 (Contract report).
798

799 **Burreson, E. M. and Andrews, J. D.** (1988). Unusual intensification of Chesapeake bay
800 oyster diseases during recent drought conditions. *OCEANS '88-A Partnership of*
801 *Marine Interests. Proceedings* (pp. 799–802) IEEE. doi:
802 10.1109/OCEANS.1988.794899.
803

804 **Burreson, E. M., Alvarez, R. S., Martinez, W. and Macedo, L. A.** (1994). *Perkinsus-*
805 *marinus* (Apicomplexa) as a potential source of oyster *Crassostrea virginica*

806 mortality in coastal lagoons of Tabasco, Mexico. *Diseases of aquatic organisms* **20**,
807 77. doi: 10.3354/dao020077.

808

809 **Bushek, D., Ford, S. E. and Allen Jr, S. K.** (1994). Evaluation of methods using Ray's
810 fluid thioglycollate medium for diagnosis of *Perkinsus marinus* infection in the
811 eastern oyster, *Crassostrea virginica*. *Annual Review of Fish Diseases* **4**, 201–217.
812 doi: 10.1016/0959-8030(94)90029-9.

813

814 **Bushek, D., Landau, B. and Scarpa, E.** (2008). *Perkinsus chesapeaki* in stout razor clams
815 *Tagelus plebeius* from Delaware bay. *Diseases of Aquatic Organisms* **78**, 243–247.
816 doi: 10.3354/dao01871.

817

818 **Bustin, S. A., Benes, V., Garson, J. A., Hellemans, J., Huggett, J., Kubista, M., Mueller,**
819 **R., Nolan, T., Pfaffl, M. W., Shipley, G. L., Vandesompele, J. and Wittwer, C. T.**
820 (2009). The MIQE guidelines: minimum information for publication of
821 quantitative real-time PCR experiments. *Clinical Chemistry* **55**, 611–622. doi:
822 10.1373/clinchem.2008.112797.

823

824 **Casas, S. M., La Peyre, J. F., Reece, K. S., Azevedo, C. and Villalba, A.** (2002a).
825 Continuous *in vitro* culture of the carpet shell clam *Tapes decussatus* protozoan
826 parasite *Perkinsus atlanticus*. *Diseases of aquatic organisms* **52**, 217–231. doi:
827 10.3354/dao052217.

828

829 **Casas, S. M., Villalba, A. and Reece, K. S.** (2002b). Study of perkinsosis in the carpet
830 shell clam *Tapes decussatus* in Galicia (NW Spain). I. Identification of the
831 aetiological agent and *in vitro* modulation of zoosporulation by temperature and
832 salinity. *Diseases of aquatic organisms* **50**, 51–65. doi:10.3354/dao050051.

833

834 **Chambouvet, A., Gower, D. J., Jirků, M., Yabsley, M. J., Davis, A. K., Leonard, G.,**
835 **Maguire, F., Doherty-Bone, T. M., Bittencourt-Silva, G. B., Wilkinson, M. and**
836 **Richards, T. A.** (2015). Cryptic infection of a broad taxonomic and geographic

837 diversity of tadpoles by Perkinsia protists. *Proceedings of the National Academy*
838 *of Sciences* **112**, E4743–E4751. doi: 10.1073/pnas.1500163112.

839

840 **Choi, K.-S., Wilson, E. A., Lewis, D. H., Powell, E. N. and Ray, S. M.** (1989). The
841 energetic cost of *Perkinsus marinus* parasitism in oysters: quantification of the
842 thioglycollate method. 125–131.

843

844 **Cold, E. R., Freyria, N. J., Martínez Martínez, J. and Fernández Robledo, J. A.** (2016).
845 An agar-based method for plating marine protozoan parasites of the genus
846 *Perkinsus*. *PLOS ONE* **11**, e0155015. doi: 10.1371/journal.pone.0155015.

847

848 **Coss, C. A., Robledo, J. A., Ruiz, G. M. and Vasta, G. R.** (2001). Description of *Perkinsus*
849 *andrewsi* n. sp. isolated from the Baltic clam (*Macoma balthica*) by
850 characterization of the ribosomal RNA locus, and development of a species-
851 specific PCR-based diagnostic assay. *Journal of Eukaryotic Microbiology* **48**, 52–
852 61.

853

854 **Cui, Y.-Y., Ye, L.-T., Wu, L. and Wang, J.-Y.** (2018). Seasonal occurrence of *Perkinsus*
855 spp. and tissue distribution of *P. olseni* in clam (*Soletellina acuta*) from coastal
856 waters of Wuchuan County, southern China. *Aquaculture* **492**, 300–305. doi:
857 10.1016/j.aquaculture.2018.04.030.

858

859 **Da Ros, L. and Canzonier, W. J.** (1985). *Perkinsus*, a protistan threat to bivalve culture
860 in the Mediterranean basin. *Bulletin of the European Association of Fish*
861 *Pathologists* **5**, 23–27.

862

863 **Dang, C., de Montaudouin, X., Caill-Milly, N. and Trumbić, Ž.** (2010). Spatio-temporal
864 patterns of perkinsosis in the Manila clam *Ruditapes philippinarum* from
865 Arcachon Bay (SW France). *Diseases of Aquatic Organisms* **91**, 151–159. doi:
866 10.3354/dao02243.

867

- 868 **De Faveri, J., Smolowitz, R. M. and Roberts, S. B.** (2009). Development and validation
869 of a real-time quantitative PCR assay for the detection and quantification of
870 *Perkinsus marinus* in the eastern oyster, *Crassostrea virginica*. *Journal of Shellfish*
871 *Research* **28**, 459–465. doi: 10.2983/035.028.0306.
- 872
- 873 **Dhanasekaran, S., Doherty, T. M., Kenneth, J. and Group, T. T. S.** (2010). Comparison
874 of different standards for real-time PCR-based absolute quantification. *Journal of*
875 *immunological methods* **354**, 34–39. doi: 10.1016/j.jim.2010.01.004.
- 876
- 877 **Dittman, D. E., Ford, S. E. and Padilla, D. K.** (2001). Effects of *Perkinsus marinus* on
878 reproduction and condition of the eastern oyster, *Crassostrea virginica*, depend
879 on timing. *Journal of Shellfish Research* **20**, 1025–1034.
- 880
- 881 **Duffy, T., Cura, C. I., Ramirez, J. C., Abate, T., Cayo, N. M., Parrado, R., Bello, Z. D.,**
882 **Velazquez, E., Muñoz-Calderon, A., Juiz, N. A., Basile, J., Garcia, L., Riarte, A.,**
883 **Nasser, J. R., Ocampo, S. B., Yadon, Z. E., Torrico, F., de Noya, B. A., Ribeiro, I.**
884 **and Schijman, A. G.** (2013). Analytical performance of a multiplex real-time PCR
885 assay using TaqMan probes for quantification of *Trypanosoma cruzi* satellite DNA
886 in blood samples. *PLoS Neglected Tropical Diseases* **7**, e2000. doi:
887 10.1371/journal.pntd.0002000.
- 888
- 889 **Elnifro, E. M., Ashshi, A. M., Cooper, R. J. and Klapper, P. E.** (2000). Multiplex PCR:
890 optimization and application in diagnostic virology. *Clinical microbiology reviews*
891 **13**, 559–570. doi: 10.1128/CMR.13.4.559.
- 892
- 893 **European Commission - DG for health and food safety** (2018). Overview report:
894 animal health controls for bivalve mollusc aquaculture.
- 895
- 896 **Flassch, J.-P. and Leborgne, Y.** (1994). Introduction in Europe, from 1972 to 1980, of
897 the Japanese Manila clam (*Tapes philippinarum*) and the effects on aquaculture
898 production and natural settlement. In *Introductions and Transfers of Aquatic*

899 *species. Selected papers from a Symposium Held in Halifax, Nova Scotia, 12-13 June*
900 *1990.*
901

902 **Food and Agriculture Organization of the United Nations** (2018). FishStatJ -
903 Software for Fishery and Aquaculture Statistical Time Series.
904

905 **Gauthier, J. D., Miller, C. R. and Wilbur, A. E.** (2006). Taqman® mgb real-time PCR
906 approach to quantification of *Perkinsus marinus* and *Perkinsus* spp. in oysters.
907 *Journal of Shellfish Research* **25**, 619–624. doi: 10.2983/0730-
908 8000(2006)25[619:TMRPAT]2.0.CO;2.
909

910 **Goggin, C. and Lester, R.** (1995). *Perkinsus*, a protistan parasite of abalone in Australia:
911 A review. *Marine and Freshwater Research* **46**, 639. doi: 10.1071/MF9950639.
912

913 **Hamaguchi, M., Suzuki, N., Usuki, H. and Ishioka, H.** (1998). *Perkinsus* protozoan
914 infection in short-necked clam *Tapes (= Ruditapes) philippinarum* in Japan. *Fish*
915 *pathology* **33**, 473–480. doi: 10.3147/jsfp.33.473.
916

917 **Hardegen, C., Messler, S., Henrich, B., Pfeffer, K., Würthner, J. and MacKenzie, C. R.**
918 (2010). A set of novel multiplex Taqman real-time PCRs for the detection of
919 diarrhoeagenic *Escherichia coli* and its use in determining the prevalence of EPEC
920 and EAEC in a university hospital. *Annals of clinical microbiology and*
921 *antimicrobials* **9**, 5. doi: 10.1186/1476-0711-9-5.
922

923 **Harvell, C. D.** (2002). Climate warming and disease risks for terrestrial and marine
924 biota. *Science* **296**, 2158–2162. doi: 10.1126/science.1063699.
925

926 **Hohweyer, J., DumèTre, A., Aubert, D., Azas, N. and Villena, I.** (2013). Tools and
927 methods for detecting and characterizing *Giardia*, *Cryptosporidium*, and
928 *Toxoplasma* parasites in marine mollusks. *Journal of Food Protection* **76**, 1649–
929 1657. doi: 10.4315/0362-028X.JFP-13-002.

930

931 **Itoh, N., Meyer, G., Tabata, A., Lowe, G., Abbott, C. and Johnson, S.** (2013).
932 Rediscovery of the Yesso scallop pathogen *Perkinsus qugwadi* in Canada, and
933 development of PCR tests. *Diseases of Aquatic Organisms* **104**, 83–91. doi:
934 10.3354/dao02578.

935

936 **Jenkins, C., Hick, P., Gabor, M., Spiers, Z., Fell, S., Gu, X., Read, A., Go, J., Dove, M.,**
937 **O'Connor, W., Kirkland, P. and Frances, J.** (2013). Identification and
938 characterisation of an ostreid herpesvirus-1 microvariant (OsHV-1 μ -var) in
939 *Crassostrea gigas* (Pacific oysters) in Australia. *Diseases of Aquatic Organisms*
940 **105**, 109–126. doi: 10.3354/dao02623.

941

942 **Kuhar, U., Barlič-Maganja, D. and Grom, J.** (2013). Development and validation of
943 TaqMan probe based real time PCR assays for the specific detection of genotype A
944 and B small ruminant lentivirus strains. *BMC veterinary research* **9**, 172. doi:
945 10.1186/1746-6148-9-172.

946

947 **Langton, S. D., Chevennement, R., Nagelkerke, N. and Lombard, B.** (2002). Analysing
948 collaborative trials for qualitative microbiological methods: accordance and
949 concordance. *International Journal of Food Microbiology* **79**, 175–181. doi:
950 10.1016/S0168-1605(02)00107-1.

951

952 **Lee, M.-K., Cho, B.-Y., Lee, S.-J., Kang, J.-Y., Jeong, H. D., Huh, S. H. and Huh, M.-D.**
953 (2001). Histopathological lesions of Manila clam, *Tapes philippinarum*, from
954 Hadong and Namhae coastal areas of Korea. *Aquaculture* **201**, 199–209. doi:
955 10.1016/S0044-8486(01)00648-2.

956

957 **Ludwig, W., Strunk, O., Westram, R., Richter, L., Meier, H., Yadhukumar, Buchner,**
958 **A., Lai, T., Steppi, S., Jobb, G., Förster, W., Brettske, I., Gerber, S., Ginhart, A.**
959 **W., Gross, O., Grumann, S., Hermann, S., Jost, R., König, A., Liss, T., Lüßmann,**
960 **R., May, M., Nonhoff, B., Reichel, B., Strehlow, R., Stamatakis, A., Stuckmann,**

961 **N., Vilbig, A., Lenke, M., Ludwig, T., Bode, A. and Schleifer, K.** (2004). ARB: a
962 software environment for sequence data. *Nucleic Acids Research* **32**, 1363–1371.
963 doi: 10.1093/nar/gkh293.

964

965 **Mackin, J. G.** (1951). Histopathology of infection of *Crassostrea virginica* (Gmelin) by
966 *Dermocystidium marinum* Mackin, Owen, and Collier. *Bulletin of Marine Science* **1**,
967 72–87.

968

969 **Mackin, J. G., Owen, H. M. and Collier, A.** (1950). Preliminary note on the occurrence of
970 a new protistan parasite, *Dermocystidium marinum* n. sp. in *Crassostrea virginica*
971 (Gmelin). *Science* **111**, 328. doi: 10.1126/science.111.2883.328.

972

973 **Marquis, N. D., Bishop, T. J., Record, N. R., Countway, P. D. and Fernández Robledo,**
974 **J. A.** (2020). A qPCR-based survey of *Haplosporidium nelsoni* and *Perkinsus* spp. in
975 the Eastern oyster, *Crassostrea virginica* in Maine, USA. *Pathogens* **9**, 256. doi:
976 10.3390/pathogens9040256.

977

978 **Montes, J., Durfort, M. and García-Valero, J.** (2001). Parasitism by the protozoan
979 *Perkinsus atlanticus* favours the development of opportunistic infections. *Diseases*
980 *of Aquatic Organisms* **46**, 57–66. doi: 10.3354/dao046057.

981

982 **Nam, K.-W., Jeung, H.-D., Song, J.-H., Park, K.-H., Choi, K.-S. and Park, K.-I.** (2018).
983 High parasite burden increases the surfacing and mortality of the Manila clam
984 (*Ruditapes philippinarum*) in intertidal sandy mudflats on the west coast of Korea
985 during hot summer. *Parasites & Vectors* **11**. doi: 10.1186/s13071-018-2620-3.

986

987 **Novoa, B., Ordás, M. C. and Figueras, A.** (2002). Hypnospores detected by RFTM in
988 clam (*Ruditapes decussatus*) tissues belong to two different protozoan organisms,
989 *Perkinsus atlanticus* and a *Perkinsus*-like organism. *Aquaculture* **209**, 11–18. doi:
990 10.1016/S0044-8486(01)00803-1.

991

- 992 **OIE** (2019a). Aquatic Animal Health Code (2019).
993
- 994 **OIE** (2019b). Chapter 2.4.7. - Infection with *Perkinsus olsenii*. *Manual of Diagnostic Tests*
995 *for Aquatic Animals*.
996
- 997 **Pagenkopp Lohan, K. M., Hill-Spanik, K. M., Torchin, M. E., Fleischer, R. C., Carnegie,**
998 **R. B., Reece, K. S. and Ruiz, G. M.** (2018). Phylogeography and connectivity of
999 molluscan parasites: *Perkinsus* spp. in Panama and beyond. *International Journal*
1000 *for Parasitology* **48**, 135–144. doi: 10.1016/j.ijpara.2017.08.014.
1001
- 1002 **Park, K.-I. and Choi, K.-S.** (2001). Spatial distribution of the protozoan parasite
1003 *Perkinsus* sp. found in the Manila clams, *Ruditapes philippinarum*, in Korea.
1004 *Aquaculture* **203**, 9–22. doi: 10.1016/S0044-8486(01)00619-6.
1005
- 1006 **Pretto, T., Zambon, M., Civettini, M., Caburlotto, G., Boffo, L., Rossetti, E. and**
1007 **Arcangeli, G.** (2014). Massive mortality in Manila clams (*Ruditapes*
1008 *philippinarum*) farmed in the Lagoon of Venice, caused by *Perkinsus olsenii*.
1009 *Bulletin- European Association of Fish Pathologists* **34**, 43–53.
1010
- 1011 **Putaporntip, C., Hongsriruang, T., Seethamchai, S., Kobasa, T., Limkittikul, K., Cui,**
1012 **L. and Jongwutiwes, S.** (2009). Differential prevalence of *Plasmodium* infections
1013 and cryptic *Plasmodium knowlesi* malaria in humans in Thailand. *The Journal of*
1014 *Infectious Diseases* **199**, 1143–1150. doi: 10.1086/597414.
1015
- 1016 **Ramilo, A., Pintado, J., Villalba, A. and Abollo, E.** (2016). *Perkinsus olsenii* and *P.*
1017 *chesapeaki* detected in a survey of perkinsosis of various clam species in Galicia
1018 (NW Spain) using PCR–DGGE as a screening tool. *Journal of invertebrate*
1019 *pathology* **133**, 50–58. doi: 10.1016/j.jip.2015.11.012.
1020

- 1021 **Ray, S. M.** (1952). A culture technique for the diagnosis of infections with
1022 *Dermocystidium marinum* (Mackin, Owen, and Collier) in oysters. *Science* **116**,
1023 360. doi: 10.1126/science.116.3014.360.
1024
- 1025 **Reece, K., Dungan, C. and Burreson, E.** (2008). Molecular epizootiology of *Perkinsus*
1026 *marinus* and *P. chesapeaki* infections among wild oysters and clams in
1027 Chesapeake bay, USA. *Diseases of Aquatic Organisms* **82**, 237–248. doi:
1028 10.3354/dao01997.
1029
- 1030 **Renault, T., Le Deuff, R.-M., Lipart, C. and Delsert, C.** (2000). Development of a PCR
1031 procedure for the detection of a herpes-like virus infecting oysters in France.
1032 *Journal of Virological Methods* **88**, 41–50. doi: 10.1016/S0166-0934(00)00175-0.
1033
- 1034 **Ríos, R., Aranguren, R., Gastaldelli, M., Arcangeli, G., Novoa, B. and Figueras, A.**
1035 (2020). Development and validation of a specific real-time PCR assay for the
1036 detection of the parasite *Perkinsus olseni*. *Journal of Invertebrate Pathology* **169**,
1037 107301. doi: 10.1016/j.jip.2019.107301.
1038
- 1039 **Ruano, F. and Cachola, R.** (1986). Outbreak of a severe epizootic of *Perkinsus marinus*
1040 (Levin-78) at Ria de Faro clam's culture beds. In *Proceedings of 2nd International*
1041 *Colloque Pathology Marine Aquatic*, pp. 4–42.
1042
- 1043 **Shamal, P., Zacharia, P. U., Binesh, C. P., Pranav, P., Suja, G., Asokan, P. K., Pradeep,**
1044 **M. A., Rithesh, R., Vijayan, K. K. and Sanil, N. K.** (2018). *Perkinsus olseni* in the
1045 short neck yellow clam, *Paphia malabarica* (Chemnitz, 1782) from the southwest
1046 coast of India. *Journal of Invertebrate Pathology* **159**, 113–120. doi:
1047 10.1016/j.jip.2018.10.001.
1048
- 1049 **Takahashi, M., Yoshinaga, T., Waki, T., Shimokawa, J. and Ogawa, K.** (2009).
1050 Development of a PCR-RFLP method for differentiation of *Perkinsus olseni* and *P.*

1051 *honshuensis* in the Manila clam *Ruditapes philippinarum*. *Fish Pathology* **44**, 185–
1052 188. doi: 10.3147/jsfp.44.185.

1053

1054 **Tall, B. D., La Peyre, J. F., Bier, J. W., Miliotis, M. D., Hanes, D. E., Kothary, M. H., Shah,**
1055 **D. B. and Faisal, M.** (1999). *Perkinsus marinus* extracellular protease modulates
1056 survival of *Vibrio vulnificus* in eastern oyster (*Crassostrea virginica*) hemocytes.
1057 *Applied and Environmental Microbiology* **65**, 4261–4263. doi:
1058 10.1128/AEM.65.9.4261-4263.1999.

1059

1060 **Ulrich, P. N., Ewart, J. W. and Marsh, A. G.** (2007). Prevalence of *Perkinsus marinus*
1061 (Dermo), *Haplosporidium nelsoni* (MSX), and QPX in bivalves of Delaware's inland
1062 bays and quantitative, high-throughput diagnosis of Dermo by qPCR. *The Journal*
1063 *of Eukaryotic Microbiology*, doi: 10.1111/j.1550-7408.2007.00293.x.

1064

1065 **Umeda, K. and Yoshinaga, T.** (2012). Development of real-time PCR assays for
1066 discrimination and quantification of two *Perkinsus* spp. in the Manila clam
1067 *Ruditapes philippinarum*. *Diseases of Aquatic Organisms* **99**, 215–225. doi:
1068 10.3354/dao02476.

1069

1070 **Untergasser, A., Cutcutache, I., Koressaar, T., Ye, J., Faircloth, B. C., Remm, M. and**
1071 **Rozen, S. G.** (2012). Primer3—new capabilities and interfaces. *Nucleic Acids*
1072 *Research* **40**, e115–e115. doi: 10.1093/nar/gks596.

1073

1074 **Wang, Y., Yoshinaga, T. and Itoh, N.** (2018). New insights into the entrance of *Perkinsus*
1075 *olseni* in the Manila clam, *Ruditapes philippinarum*. *Journal of Invertebrate*
1076 *Pathology* **153**, 117–121. doi: 10.1016/j.jip.2018.03.005.

1077

1078 **Ward, J. R. and Lafferty, K. D.** (2004). The elusive baseline of marine disease: are
1079 diseases in ocean ecosystems increasing? *PLoS biology* **2**. doi:
1080 10.1371/journal.pbio.0020120.

1081

1082 **Winnepenninckx, B., Backeljau, T. and De Wachter, R.** (1993). Extraction of high
1083 molecular weight DNA from molluscs. *Trends in Genetics* **9**, 407.
1084

1085 **Xie, Z., Xie, L., Fan, Q., Pang, Y., Deng, X., Xie, Z. Q., Liu, J. and Khan, M. I.** (2013). A
1086 duplex quantitative real-time PCR assay for the detection of *Haplosporidium* and
1087 *Perkinsus* species in shellfish. *Parasitology Research* **112**, 1597–1606. doi:
1088 10.1007/s00436-013-3315-5.
1089

1090 **Yarnall, H. A., Reece, K. S., Stokes, N. A. and Bureson, E. M.** (2000). A quantitative
1091 competitive polymerase chain reaction assay for the oyster pathogen *Perkinsus*
1092 *marinus*. *Journal of Parasitology* **86**, 827–837. doi: 10.1645/0022-
1093 3395(2000)086[0827:AQCPCR]2.0.CO;2.
1094

Figure 1. Schematic position of primers and probes designed for duplex TaqMan PCR within the ITS1-5.8S-ITS2 sequence region of ribosomal genes of *Perkinsus* spp.

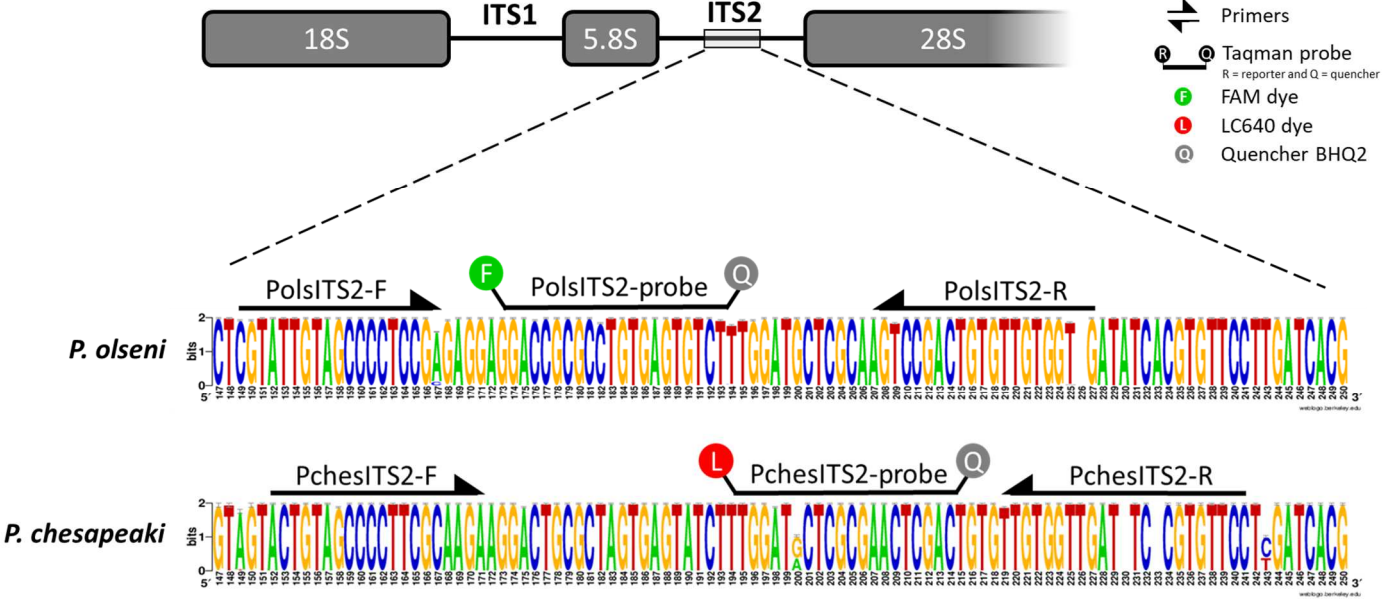


Figure 2. Specificity of primers and probes designed for the duplex qPCR assay. Primers and probes specificity were tested by conducting duplex real-time PCR on *P. olseni* gDNA (1 pg), *P. chesapeaki* gDNA (1 pg), *R. philippinarum* gills gDNA (50 ng) and pure water. Positive amplification is significant when the fluorescence values exceed the threshold indicated by the horizontal red line. Amplification curves demonstrating the specificity of *P. olseni* primers on *P. olseni* gDNA between 465-510 nm and the specificity of *P. chesapeaki* set on *P. chesapeaki* gDNA between 618-660 nm. NTC: Non-Template Control (water).

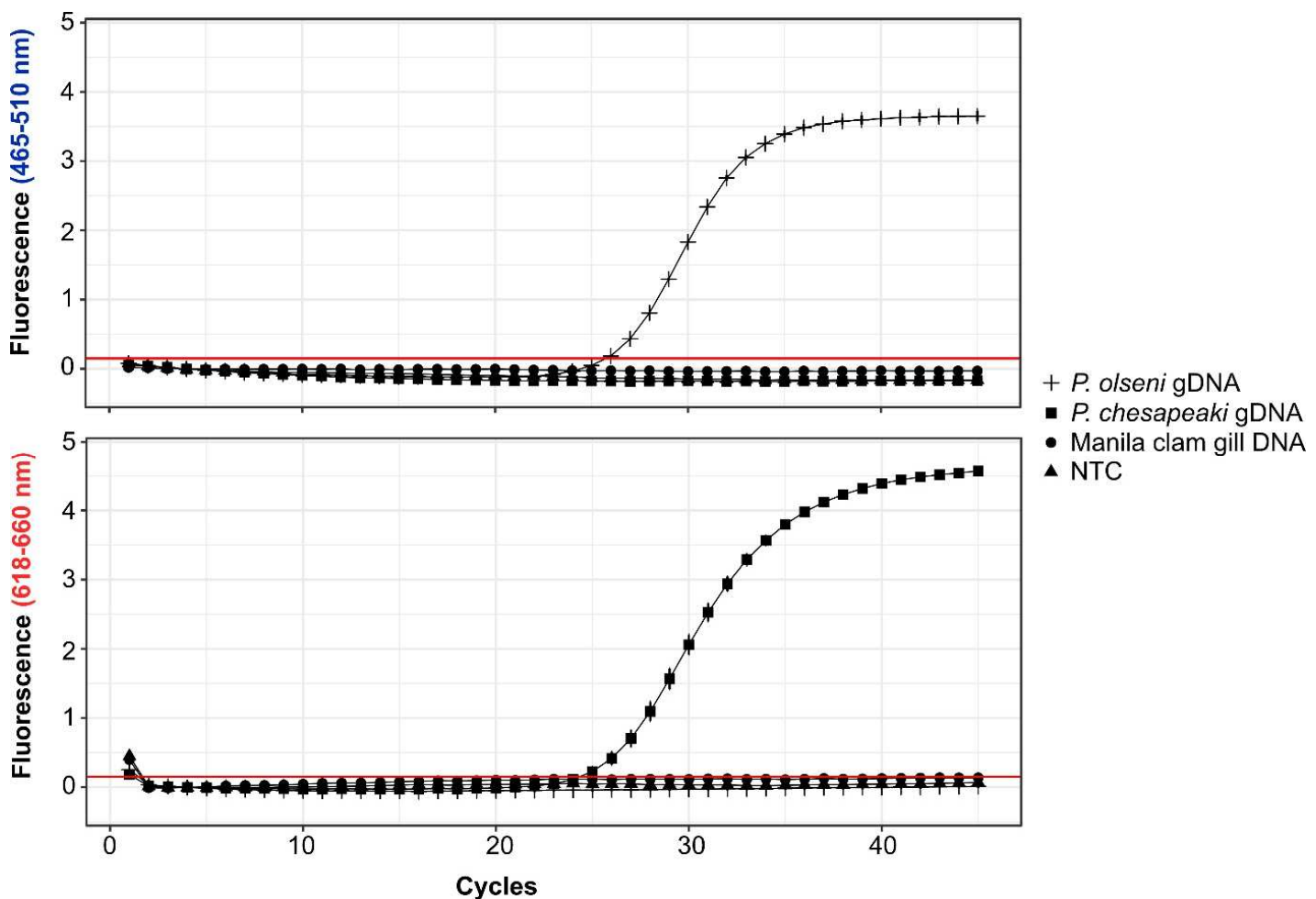


Figure 3. Standards and efficiency evaluation of real-time PCR assays. Standard curves based on *P. olseni*-plasmids and on *P. chesapeakei*-plasmids serial dilution were determined for downstream analysis. *P. olseni* standard relationship: $y = -3.33x + 39.48$; *P. chesapeakei* standard relationship: $y = -3.38x + 40.30$ Ct: Cycle threshold value. E: Efficiency (E) of the qPCR assay is calculated as follow: $E = (10^{(-1/\text{slope})} - 1) \times 100\%$.

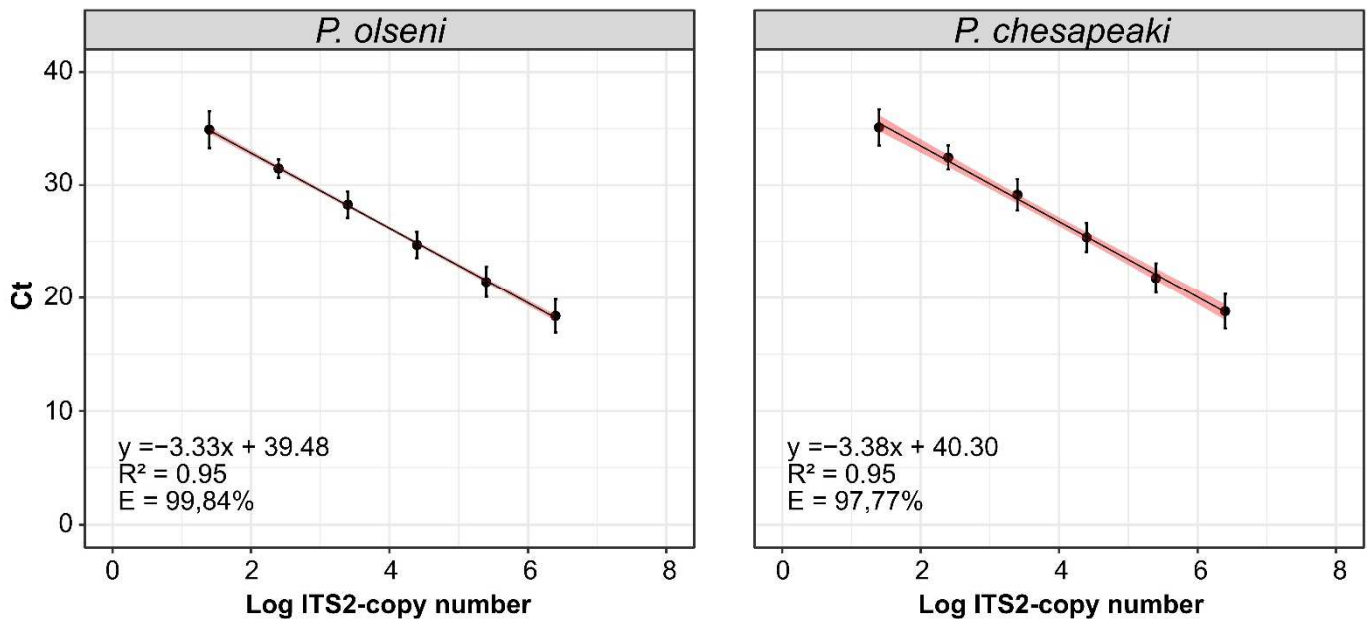


Figure 4. Sensitivity and inhibitory effects induced by four concentrations of gDNA from the six different types of tissue samples (gill, digestive gland, adductor muscle, foot, mantle and remaining tissue). The sensitivity of the real-time duplex PCR is represented for six (A) *P. olseni*-plasmids and (B) *P. chesapeaki*-plasmids dilution combined with four gDNA concentrations: 2 ng.μl⁻¹, 5 ng.μl⁻¹, 10 ng.μl⁻¹ and 20 ng.μl⁻¹. The specific standard curve is represented by the red curve with round red circles. Ct: Cycle threshold value.

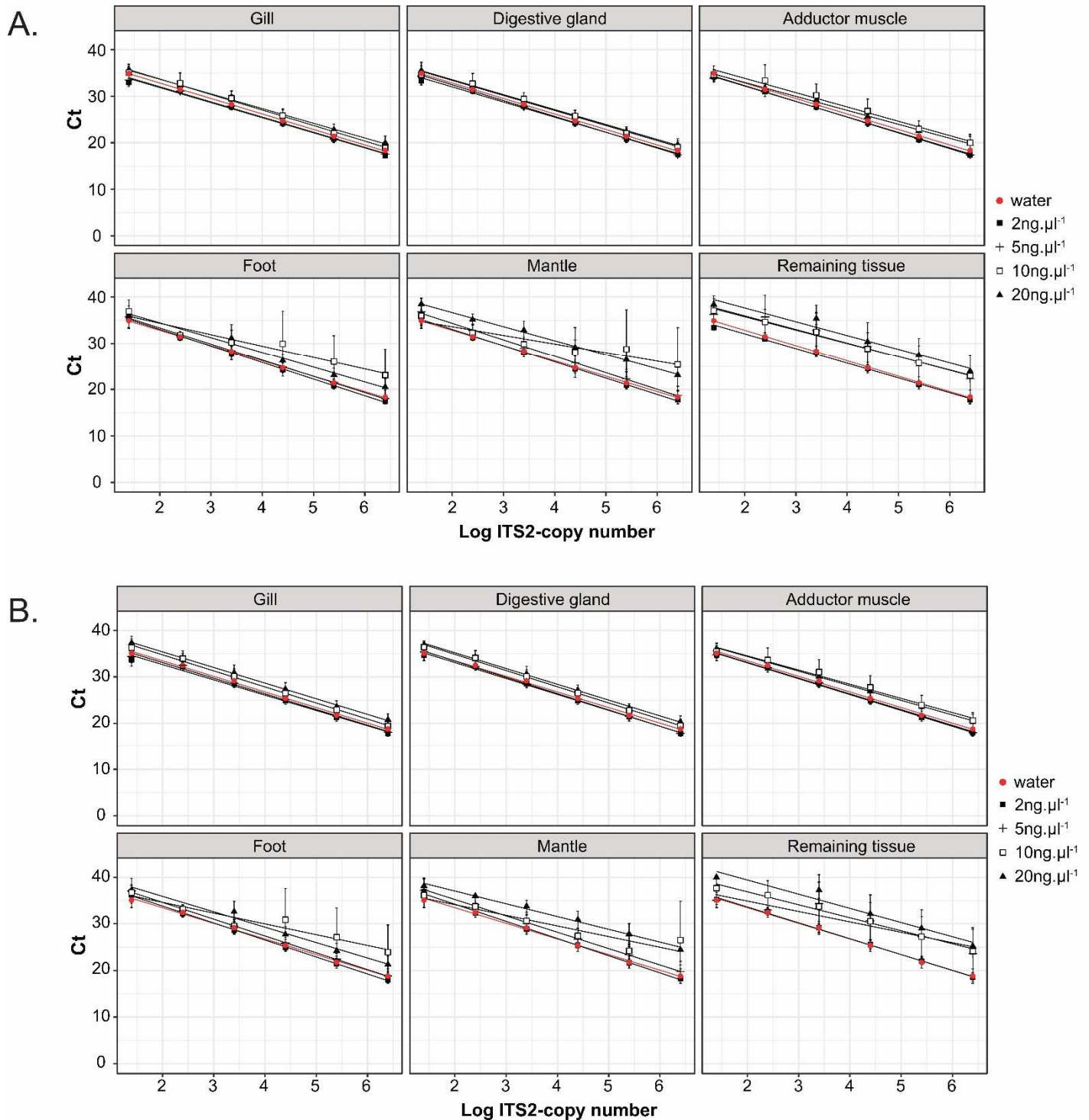


Figure 5. Linear regression between infection intensities determined by RFTM assay (nb. of cells.g of wet gill⁻¹) and by qPCR assay (nb. of copies.g of wet gill⁻¹). The infection intensities determined by RFTM are based on the global counting of *Perkinsus* sp. hypnospores. The infection intensities determined by duplex qPCR are based on the sum of *P. olseni* and *P. chesapeakei* copies. RFTM and qPCR relationship: $y = -0.60x + 4.36$. Ct: Cycle threshold value. r: Pearson's coefficient.

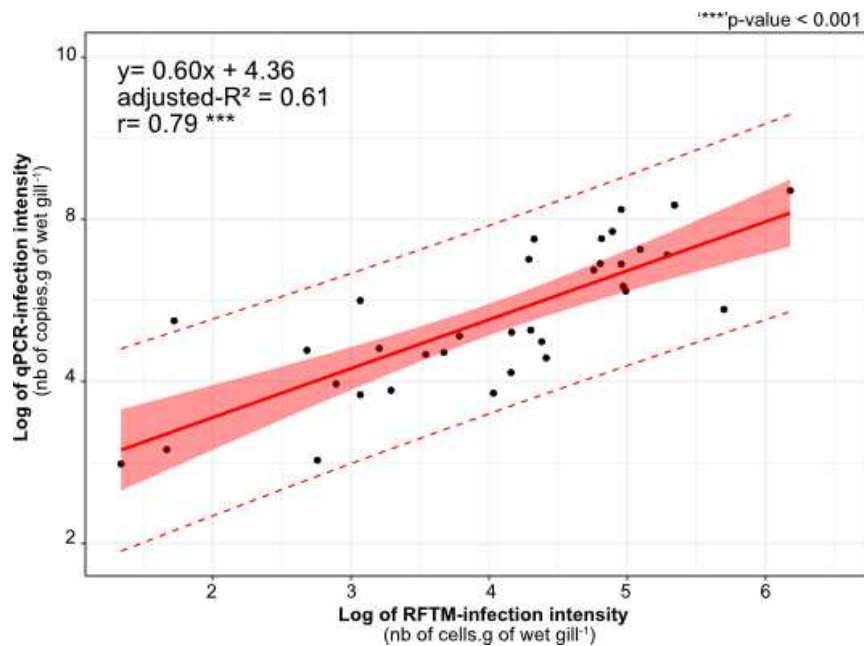


Figure S1. Map of the sampling site in Arcachon Bay (SW France, Atlantic coast, 44°41'60" N; 1°10' W) indicating the collecting point at Lanton.

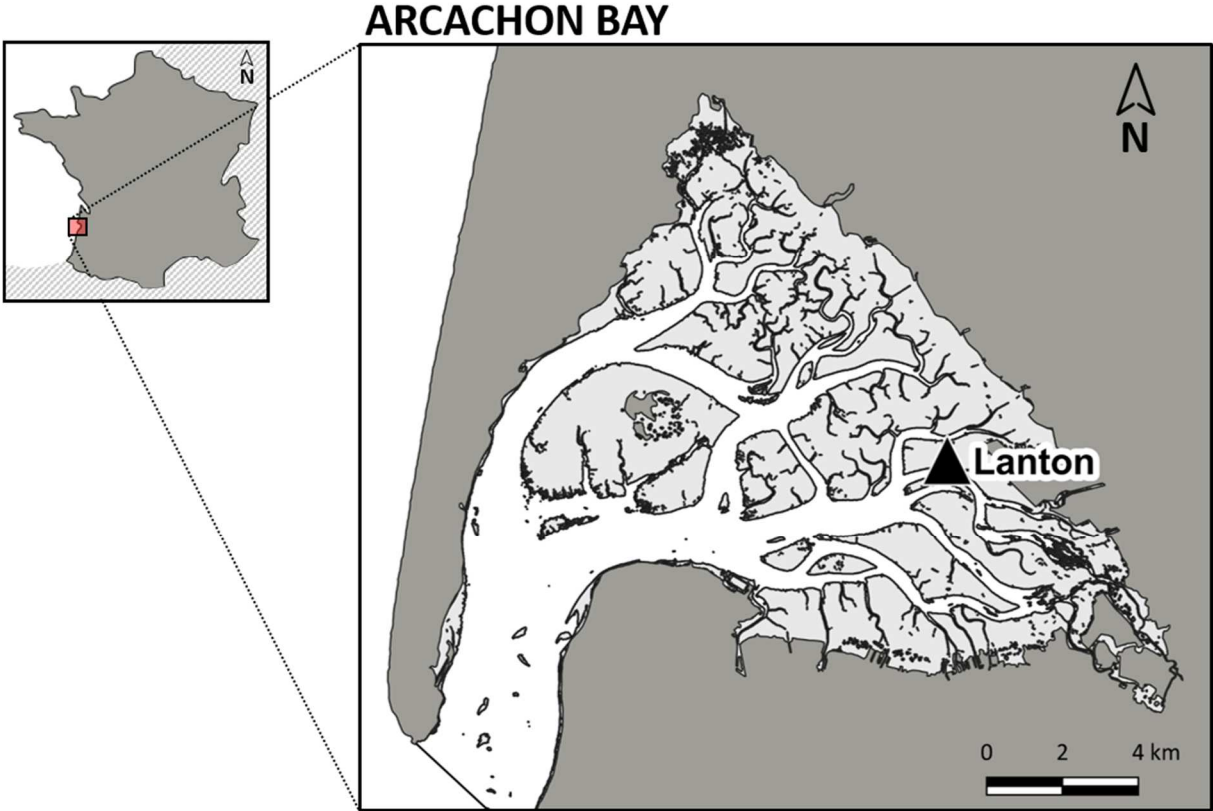


Figure S2. Neighbour joining (NJ) tree of *Perkinsus* genus diversity using the ITS1-5.8S-ITS2 region of the ribosomal operon. The phylogeny was calculated from 57 taxa and 633 characters alignment position. NJ distances (1000 replicates), Maximum Likelihood (ML) bootstraps (1000 replicates) and Bayesian posterior probability (2,000,000 generations, HKY+G model) were added at each node as follows: black circle: bootstrap values are equal to or higher than 80%/80%/0.8; white circle: bootstrap values are higher than 60%/60%/0.6; '+': bootstrap value is below 60% or 600 and if the topology is consistent; '-': the topology is not consistent. The double-slides means the branch has been reduced by two. Five sequences of *P. qugwadi* were used as an outgroup.

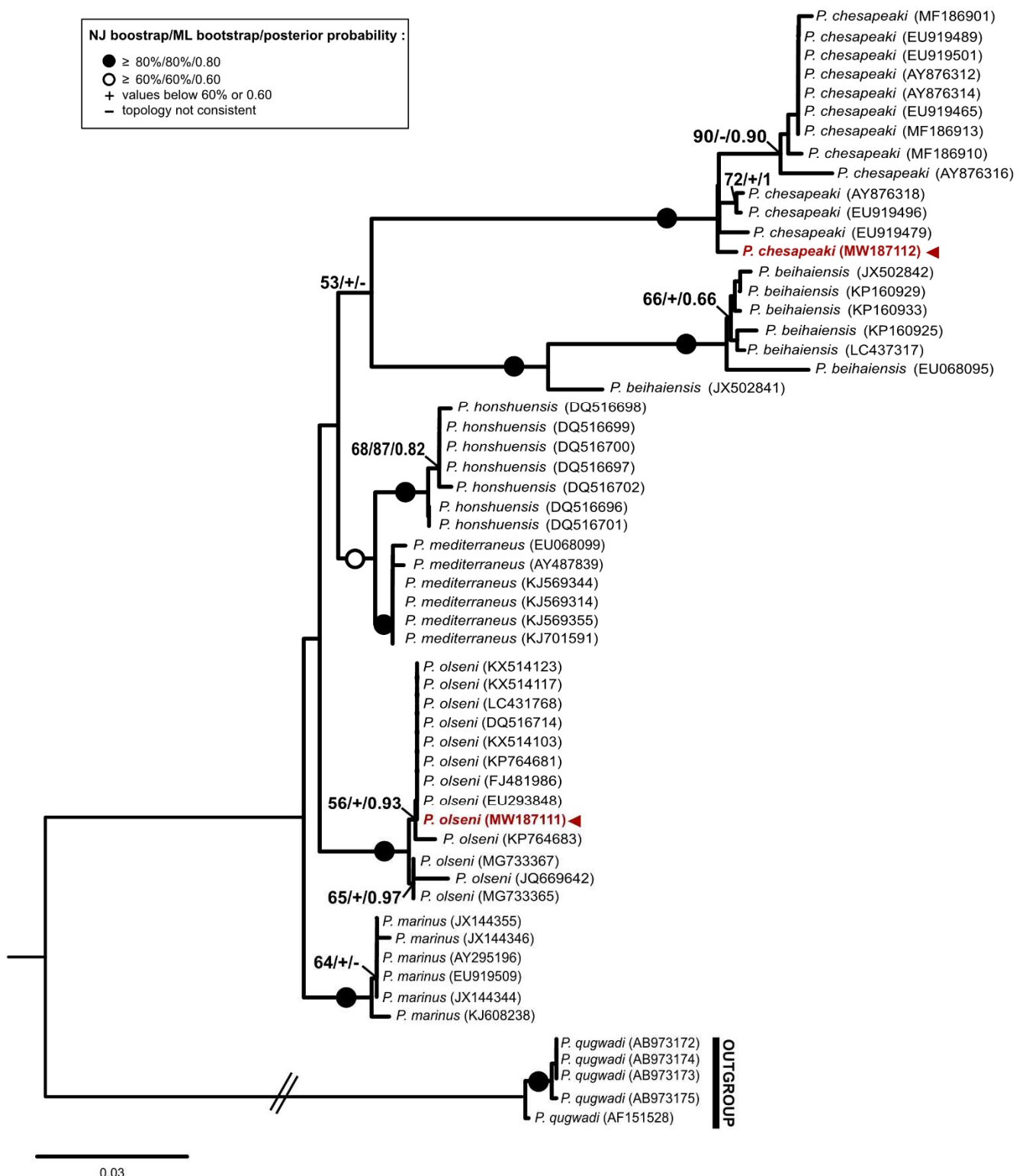


Table 1. Primer and probe sequences specific to *P. olseni* and *P. chesapeaki* ITS2 sequence region of nuclear ribosomal DNA. Excitation wavelengths of FAM fluorochrome is 465-510 nm and of LC640 fluorochrome is 618-660 nm.

Target	Primer /probe	Sequence (5'->3')	Tm (°C)	Amplicon size
ITS 2 <i>P. olseni</i>	PolsITS2-F	CACCACAACACAGTCGGAC	58,8	76 bp
	PolsITS2-R	CGTATTGTAGCCCCTCCGA	58,8	
	PolsITS2-probe	FAM -GACTCTCACAGGCGCGGTCC- [BHQ2]	65,7	
ITS 2 <i>P. chesapeaki</i>	PchesITS2-F	GGAACACGGAATCAACCACA	57,3	87 bp
	PchesITS2-R	ACTGTAGCCCCTTCGCAAG	58,8	
	PchesITS2-probe	LC640 -AGTCGAGTTCGCGAGCATCCAA- [BHQ2]	63,3	

Table 2. Repeatability of the duplex qPCR assay estimated by the coefficient of variation (CV; %) for *P. olseni* and *P. chesapeakei* plasmid standard concentrations (from 2.5×10^1 to 2.5×10^6 copies).

	number of copies					
	2.5×10^1	2.5×10^2	2.5×10^3	2.5×10^4	2.5×10^5	2.5×10^6
<i>P. olseni</i> standard	5 %	3 %	4 %	5 %	6 %	8 %
<i>P. chesapeakei</i> standard	5 %	3 %	5 %	5 %	6 %	8 %

Table 3. Comparison of Perkinsosis prevalences on gill tissue samples at Lanton determined by the standard RFTM methodology and the duplex qPCR methodology. Unq.: unquantifiable.

Type of method	nb. of clams tested	nb. of infected clams	nb. of healthy clams	Prevalence (%)				
				<i>Perkinsus</i> sp.	<i>P. olseni</i>	<i>P. chesapeakei</i>	Single-infection	Co-infection
RFTM	50	37	13	74	Unq.	Unq.	Unq.	Unq.
duplex qPCR	50	37	13	74	74	6	68	6

Table 4. Concordance parameters of duplex qPCR method and RFTM method. The a, b, c and d are expressed as number of individuals based on a total of 50 clams (n).

		RFTM assay				
		positive	negative	Concordance	a+d/n	88 %
Duplex qPCR assay	positive	34 (a)	3 (b)	Discordance	b+c/n	12 %
	negative	3 (c)	10 (d)			

Table S1. Characteristic of the Perkinsosis at Lanton station. 'n', is the number of Manila clams sampled in each station. Prevalence is estimated using the RFTM/NaOH digestion methodology (Choi *et al.*, 1989) and represents the number of infected clams on the total of clams sampled (%). The infection intensity is calculated by the mean of the number of hypnospores per gram of wet gill weight (g) in infected hosts. SD, is the standard-deviation. nd: not determined.

Site	Latitude (X)	Longitude (Y)	Type of analysis	n	Prevalence RFTM (%)	Mean infection intensity (nb. of cells.g ⁻¹ of wet tissue ± SD)
Lanton	44°41'31"N	1°4'48"W	Perkinsosis diagnostis	50	74	9.07x10 ⁴ ± 2.24x10 ⁵
			Culture	5	100	nd

Table S2. GenBank ITS1-5.8S-ITS2 sequence region belonging to *Perkinsus* genus used in phylogenetic analysis to design and test *P. olseni* and *P. chesapeaki* specific primers and probes in duplex qPCR assays.

Accession no.	Class	Order	Genus	Species	Strain/Clone	Reference
JX144346	Perkinsea	Perkinsida	<i>Perkinsus</i>	<i>marinus</i>	60_2	(da Silva <i>et al.</i> , 2013)
KJ608238	Perkinsea	Perkinsida	<i>Perkinsus</i>	<i>marinus</i>	70_3_C_c5	(da Silva <i>et al.</i> , 2014)
JX144355	Perkinsea	Perkinsida	<i>Perkinsus</i>	<i>marinus</i>	69	(da Silva <i>et al.</i> , 2013)
EU919509	Perkinsea	Perkinsida	<i>Perkinsus</i>	<i>marinus</i>	PXBICv25-B9-C5	(Reece <i>et al.</i> , 2008)
AY295196	Perkinsea	Perkinsida	<i>Perkinsus</i>	<i>marinus</i>	SC2_4_7	(Brown <i>et al.</i> , 2004)
JX144344	Perkinsea	Perkinsida	<i>Perkinsus</i>	<i>marinus</i>	60	(da Silva <i>et al.</i> , 2013)
KJ569344	Perkinsea	Perkinsida	<i>Perkinsus</i>	<i>mediterraneus</i>	H08_3_06	(Valencia <i>et al.</i> , 2014)
AY487839	Perkinsea	Perkinsida	<i>Perkinsus</i>	<i>mediterraneus</i>	D10	(Casas <i>et al.</i> , 2004)
KJ569314	Perkinsea	Perkinsida	<i>Perkinsus</i>	<i>mediterraneus</i>	H03_3_04	(Valencia <i>et al.</i> , 2014)
KJ569355	Perkinsea	Perkinsida	<i>Perkinsus</i>	<i>mediterraneus</i>	H03_28_A3	(Valencia <i>et al.</i> , 2014)
EU068099	Perkinsea	Perkinsida	<i>Perkinsus</i>	<i>mediterraneus</i>	Jer2_50	(Casas <i>et al.</i> , 2008)
KJ701591	Perkinsea	Perkinsida	<i>Perkinsus</i>	<i>mediterraneus</i>	12	(Ramilo <i>et al.</i> , 2015)
DQ516701	Perkinsea	Perkinsida	<i>Perkinsus</i>	<i>honshuensis</i>	Mie3gH8_3	(Dungan and Reece, 2006)
DQ516696	Perkinsea	Perkinsida	<i>Perkinsus</i>	<i>honshuensis</i>	Mie3g_2	(Dungan and Reece, 2006)
DQ516702	Perkinsea	Perkinsida	<i>Perkinsus</i>	<i>honshuensis</i>	Mie3gH8_4	(Dungan and Reece, 2006)
DQ516699	Perkinsea	Perkinsida	<i>Perkinsus</i>	<i>honshuensis</i>	Mie3gH8_1	(Dungan and Reece, 2006)
DQ516700	Perkinsea	Perkinsida	<i>Perkinsus</i>	<i>honshuensis</i>	Mie3gH8_2	(Dungan and Reece, 2006)
DQ516698	Perkinsea	Perkinsida	<i>Perkinsus</i>	<i>honshuensis</i>	Mie3g_4	(Dungan and Reece, 2006)
DQ516697	Perkinsea	Perkinsida	<i>Perkinsus</i>	<i>honshuensis</i>	Mie3g_3	(Dungan and Reece, 2006)
JX502841	Perkinsea	Perkinsida	<i>Perkinsus</i>	<i>beihaiensis</i>	138	(Sabry <i>et al.</i> , 2013)
KP160933	Perkinsea	Perkinsida	<i>Perkinsus</i>	<i>beihaiensis</i>	CBMA287	(Queiroga <i>et al.</i> , 2015) Itoh <i>et al.</i> 2019
LC437317	Perkinsea	Perkinsida	<i>Perkinsus</i>	<i>beihaiensis</i>	Koitogawa_4	unpublished
KP160925	Perkinsea	Perkinsida	<i>Perkinsus</i>	<i>beihaiensis</i>	CBMA92	(Queiroga <i>et al.</i> , 2015)
KP160929	Perkinsea	Perkinsida	<i>Perkinsus</i>	<i>beihaiensis</i>	CBMA142	(Queiroga <i>et al.</i> , 2015)
JX502842	Perkinsea	Perkinsida	<i>Perkinsus</i>	<i>beihaiensis</i>	34	(Sabry <i>et al.</i> , 2013)
EU068095	Perkinsea	Perkinsida	<i>Perkinsus</i>	<i>beihaiensis</i>	QZ0649	(Moss <i>et al.</i> , 2008)
AB973173	Perkinsea	Perkinsida	<i>Perkinsus</i>	<i>qugwadi</i>	8302-1	(Itoh <i>et al.</i> , 2013)
AB973174	Perkinsea	Perkinsida	<i>Perkinsus</i>	<i>qugwadi</i>	8302-11	(Itoh <i>et al.</i> , 2013)
AB973175	Perkinsea	Perkinsida	<i>Perkinsus</i>	<i>qugwadi</i>	8302-51	(Itoh <i>et al.</i> , 2013)
AB973172	Perkinsea	Perkinsida	<i>Perkinsus</i>	<i>qugwadi</i>	6675-2	(Itoh <i>et al.</i> , 2013)
AF151528	Perkinsea	Perkinsida	<i>Perkinsus</i>	<i>qugwadi</i>	-	Hervio <i>et al.</i> 1999 unpublished
EU919479	Perkinsea	Perkinsida	<i>Perkinsus</i>	<i>chesapeaki</i>	EBNPMb2-B5-D12	(Reece <i>et al.</i> , 2008)
EU919489	Perkinsea	Perkinsida	<i>Perkinsus</i>	<i>chesapeaki</i>	PXBIMa10-D10-E4	(Reece <i>et al.</i> , 2008)
EU919501	Perkinsea	Perkinsida	<i>Perkinsus</i>	<i>chesapeaki</i>	YRKCMb1-G2-G8	(Reece <i>et al.</i> , 2008)
AY876312	Perkinsea	Perkinsida	<i>Perkinsus</i>	<i>chesapeaki</i>	ATCC 50807	(Burreson <i>et al.</i> , 2005)
AY876314	Perkinsea	Perkinsida	<i>Perkinsus</i>	<i>chesapeaki</i>	ATCC 50807	(Burreson <i>et al.</i> , 2005)

EU919465	Perkinsea	Perkinsida	<i>Perkinsus</i>	<i>chesapeaki</i>	CRBSTp9	(Reece <i>et al.</i> , 2008)
EU919496	Perkinsea	Perkinsida	<i>Perkinsus</i>	<i>chesapeaki</i>	PXSATp6-A7-A8	(Reece <i>et al.</i> , 2008)
AY876318	Perkinsea	Perkinsida	<i>Perkinsus</i>	<i>chesapeaki</i>	ATCC PRA-65	(Burreson <i>et al.</i> , 2005)
AY876316	Perkinsea	Perkinsida	<i>Perkinsus</i>	<i>chesapeaki</i>	ATCC PRA-65	(Burreson <i>et al.</i> , 2005)
MF186901	Perkinsea	Perkinsida	<i>Perkinsus</i>	<i>chesapeaki</i>	A9-1	(Reece <i>et al.</i> , 2017)
MF186913	Perkinsea	Perkinsida	<i>Perkinsus</i>	<i>chesapeaki</i>	A5_4	(Reece <i>et al.</i> , 2017)
MF186910	Perkinsea	Perkinsida	<i>Perkinsus</i>	<i>chesapeaki</i>	A7_2	(Reece <i>et al.</i> , 2017)
JQ669642	Perkinsea	Perkinsida	<i>Perkinsus</i>	<i>olseni</i>	05067_3P2/1_6	(Arzul <i>et al.</i> , 2012) Cho <i>et al.</i> 2018 unpublished
KX514117	Perkinsea	Perkinsida	<i>Perkinsus</i>	<i>olseni</i>	MS2-2	Cho <i>et al.</i> 2018 unpublished
KX514123	Perkinsea	Perkinsida	<i>Perkinsus</i>	<i>olseni</i>	SS2-2	Imajoh <i>et al.</i> 2018 unpublished
LC431768	Perkinsea	Perkinsida	<i>Perkinsus</i>	<i>olseni</i>	shoG	unpublished (Dungan and Reece, 2006)
DQ516714	Perkinsea	Perkinsida	<i>Perkinsus</i>	<i>olseni</i>	Mie13v_8	(Shamal <i>et al.</i> , 2018)
MG733367	Perkinsea	Perkinsida	<i>Perkinsus</i>	<i>olseni</i>	PM51DH1	(Shamal <i>et al.</i> , 2018)
MG733365	Perkinsea	Perkinsida	<i>Perkinsus</i>	<i>olseni</i>	PM45EL4	(Shamal <i>et al.</i> , 2018)
KP764683	Perkinsea	Perkinsida	<i>Perkinsus</i>	<i>olseni</i>	8	(Ramilo <i>et al.</i> , 2016) Cho <i>et al.</i> 2018 unpublished
KX514103	Perkinsea	Perkinsida	<i>Perkinsus</i>	<i>olseni</i>	WD4-2	(Ramilo <i>et al.</i> , 2016)
KP764681	Perkinsea	Perkinsida	<i>Perkinsus</i>	<i>olseni</i>	6	Elandaloussi <i>et al.</i> , 2008 unpublished
FJ481986	Perkinsea	Perkinsida	<i>Perkinsus</i>	<i>olseni</i>	Rp1	(Elandaloussi <i>et al.</i> , 2009)
EU293848	Perkinsea	Perkinsida	<i>Perkinsus</i>	<i>olseni</i>	-	

Table S3. *In silico* specificity of primers using Primer-BLAST (Ye *et al.*, 2012). Sets of primers were tested against the non-redundant (nr) Genbank genetic database constraint to specific phyla: Apicomplexa, Dinoflagellata, Haplosporidians, Thraustochytridae, organisms belonging to *Parvilucifera* genus and *Perkinsus* species. Targets that had six or more mismatches to the primers were ignored. Details of targets presenting less than six mismatches are listed in the table. Number of mismatches between the target and the primer are represented by F to the forward primer and by R to the reverse primer.

Primers	Taxid	Phylum	Nb. of mismatch	Products on target templates	NCBI reference sequence	Product length (bp)	
PolsITS2_F/PolsITS2_R	330153	<i>Perkinsus chesapeaki</i>		no match sequences			
	31276	<i>Perkinsus marinus</i>	F:5, R:5	<i>Perkinsus marinus</i> ATCC 50983 hypothetical protein, mRNA	XM_002787768.1	1082	
	259652	<i>Perkinsus mediterraneus</i>		no match sequences			
	1074429	<i>Perkinsus beihaiensis</i>	F:1, R:4	<i>Perkinsus beihaiensis</i> isolate 138 et 31	JX502841.1/JX502840.1	83	
	386307	<i>Perkinsus honshuensis</i>		no match sequences			
	103982	<i>Parvilucifera</i> spp.		no match sequences			
			F:4, R:4	<i>Plasmodium knowlesi</i> strain H SICA antigen (fragment) partial mRNA	XM_002259474.1	2294	
	5794	Apicomplexa	F:5, R:4	<i>Plasmodium cynomolgi</i> genome assembly, chromosome: 7	LT841385.1	1027	
			F:5, R:4	<i>Gregarina niphandrodes</i> peptidase partial mRNA	XM_011133033.1	2460	
		2864	Dinoflagellates		no match sequences		
	31291	Haplosporidians		no match sequences			
	33674	Thraustochytridae		no match sequences			
PchesITS2_F/PchesITS2_R	32597	<i>Perkinsus olseni</i>		no match sequences			
	31276	<i>Perkinsus marinus</i>		no match sequences			
	259652	<i>Perkinsus mediterraneus</i>		no match sequences			
	1074429	<i>Perkinsus beihaiensis</i>		no match sequences			
	386307	<i>Perkinsus honshuensis</i>		no match sequences			
	103982	<i>Parvilucifera</i> spp.		no match sequences			
	5794	Apicomplexa	F:5, R:5	<i>Neospora caninum</i> Liverpool, chromosome chrXI, complete genome	LN714486.1	3944	
		2864	Dinoflagellates		no match sequences		
		31291	Haplosporidians		no match sequences		
	33674	Thraustochytridae		no match sequences			

Table S4. Ten best hits from the *in silico* specificity test of (A) *P. olseni* and (B) *P. chesapeaki* probes using Blastn against nr NCBI database (accessed March 2019) excluding the corresponding parasitic sequences respectively. Best hits were dominated by *Perkinsus* sp. sequences, marked by * down to both tables due to poor affiliation in the reference database. These sequences were fully checked using Blastn and respectively affiliated to *P. olseni* and *P. chesapeaki* species; thereafter they were discarded to the 10 Best hits.

A.

10 Best hits for <i>P. olseni</i> probe sequence						
Description	Max Score	Total Score	Query Cover	E value	Per. Ident	Accession
PREDICTED: <i>Quercus suber</i> beta-mannosidase A-like (LOC112014742), mRNA	36.2	36.2	90%	8.3	100%	XM_024047133.1
<i>Rhodococcus</i> sp. DMU1 chromosome, complete genome	34.2	34.2	85%	33	100%	CP050952.1
<i>Monaibacterium</i> sp. ALG8 chromosome, complete genome	34.2	34.2	85%	33	100%	CP049811.1
<i>Halogeometricum borinquense</i> strain wsp4 chromosome, complete genome	34.2	34.2	85%	33	100%	CP048739.1
<i>Salmo trutta</i> genome assembly, chromosome: 12	34.2	34.2	85%	33	100%	LR584441.1
<i>Salmo trutta</i> genome assembly, chromosome: 29	34.2	34.2	85%	33	100%	LR584418.1
<i>Bos mutus</i> isolate yakQH1 chromosome 22	34.2	34.2	85%	33	100%	CP027090.1
<i>Ovis canadensis canadensis</i> isolate 43U chromosome 19 sequence	34.2	34.2	85%	33	100%	CP011904.1
<i>Rhodococcus aetherivorans</i> strain IcdP1, complete genome	34.2	34.2	85%	33	100%	CP011341.1
PREDICTED: <i>Callorhinchus milii</i> cytosolic phospholipase A2 gamma-like (LOC103190768), transcript variant X1, mRNA	34.2	34.2	85%	33	100%	XM_007911657.1
* <i>Perkinsus</i> sp. : KM983404, LC524156, AF522321, U07699, U07698, KM983403, KM983402, KM983401	99.52% to 100% : <i>P. olseni</i>					

B.**10 Best hits for *P. chesapeaki* probe sequence**

Description	Max Score	Total Score	Query Cover	E value	Per. Ident	Accession
<i>Arabis alpina</i> genome assembly, chromosome: 5	40.1	40.1	90%	0.53	100%	LT669792.1
<i>Arabis alpina</i> genome assembly, chromosome: 4	40.1	152	90%	0.53	100%	LT669791.1
<i>Arabis alpina</i> genome assembly, chromosome: 2	40.1	199	90%	0.53	100%	LT669789.1
<i>Microbacterium</i> sp. SGAir0570 chromosome, complete genome	36.2	36.2	81%	8.3	100%	CP027929.1
<i>Cellulomonas shaoxiangyii</i> strain Z28 chromosome, complete genome	36.2	36.2	81%	8.3	100%	CP039291.1
<i>Halomonas alkaliphila</i> X3, complete sequence	36.2	36.2	81%	8.3	100%	CP024811.1
<i>Paenibacillus lautus</i> strain E7593-69 chromosome, complete genome	36.2	36.2	81%	8.3	100%	CP032412.1
<i>Rubrobacter indicoceani</i> strain SCSIO 08198 chromosome	36.2	36.2	81%	8.3	100%	CP031115.1
<i>Kocuria rhizophila</i> strain NCTC8340 genome assembly, chromosome: 1	36.2	36.2	81%	8.3	100%	LR134409.1
<i>Kocuria</i> sp. BT304 chromosome, complete genome	36.2	36.2	81%	8.3	100%	CP030039.1

* *Perkinsus* sp. : KM983418.1, KM983416.1, KM983415.1, KM983414.1, KM983413.1, 98.93% to 100% : *P. chesapeaki*
 KM983412.1, KM983411.1, KM983409.1, KM983407.1, KM983406.1, KM983405.1, KM983400.1,
 JQ669649.1, JQ669647.1, JQ669646.1, AF440466.1, AF440465.1, KM983408.1

Table S5. Standard curve equations, qPCR efficiencies and ANOVA-test (F) associated with p-value (significant ‘*’ 0.05, ‘**’ 0.01, ‘***’ 0.001 and not significant ‘ns’) for each condition depending on the type of organ and its concentration (ng/μl) tested on both *P. olseni*-plasmidic and *P. chesapeaki*-plasmidic serial dilutions. Red highlights represent best parameters for *P. olseni*; grey highlights represent best parameters for *P. chesapeaki*.

Species	Type of organ	Organ DNA concentration (ng/μl)	Equation curve	R ²	ANCOVA (F)	p-value	Efficiency (10 ^(-1/slope) ×100%)
<i>P. olseni</i>	Gill	2	-3.34x + 38.77	0.99	0.00	ns	99.9%
<i>P. olseni</i>	Gill	5	-3.13x + 38.82	0.99	0.01	ns	108.6%
<i>P. olseni</i>	Gill	10	-3.37x + 40.57	0.93	0.10	ns	97.9%
<i>P. olseni</i>	Gill	20	-3.32x + 39.97	0.96	1.85	ns	100.3%
<i>P. olseni</i>	Digestive gland	2	-3.32x + 38.83	0.99	0.01	ns	100.3%
<i>P. olseni</i>	Digestive gland	5	-3.43x + 39.38	1.00	0.52	ns	95.9%
<i>P. olseni</i>	Digestive gland	10	-3.28x + 40.11	0.93	0.09	ns	101.7%
<i>P. olseni</i>	Digestive gland	20	-3.31x + 39.75	0.98	0.82	ns	100.4%
<i>P. olseni</i>	Adductor muscle	2	-3.40x + 39.09	1.00	0.22	ns	97.1%
<i>P. olseni</i>	Adductor muscle	5	-3.36x + 39.00	0.99	0.04	ns	98.6%
<i>P. olseni</i>	Adductor muscle	10	-3.13x + 40.27	0.84	2.88	ns	108.7%
<i>P. olseni</i>	Adductor muscle	20	-3.00x + 38.97	0.97	5.54	*	115.4%
<i>P. olseni</i>	Foot	2	-3.57x + 40.22	0.99	4.47	*	90.6%
<i>P. olseni</i>	Foot	5	-3.51x + 40.36	0.97	1.61	ns	92.8%
<i>P. olseni</i>	Foot	10	-2.54x + 39.70	0.47	8.43	**	147.3%
<i>P. olseni</i>	Foot	20	-3.26x + 41.27	0.91	17.59	***	102.7%
<i>P. olseni</i>	Mantle	2	-3.53x + 40.07	0.99	2.43	ns	92.0%
<i>P. olseni</i>	Mantle	5	-3.57x + 41.46	0.94	2.28	ns	90.6%
<i>P. olseni</i>	Mantle	10	-1.83x + 37.25	0.24	16.04	***	252.2%
<i>P. olseni</i>	Mantle	20	-3.05x + 42.76	0.90	2.84	ns	112.9%
<i>P. olseni</i>	Remaining tissue	2	-3.19x + 38.46	0.99	1.06	ns	105.6%
<i>P. olseni</i>	Remaining tissue	5	-2.99x + 42.07	0.55	6.11	*	115.9%
<i>P. olseni</i>	Remaining tissue	10	-2.89x + 41.55	0.68	2.16	ns	121.7%
<i>P. olseni</i>	Remaining tissue	20	-3.07x + 44.28	0.93	8.71	**	111.9%
<i>P. chesapeaki</i>	Gill	2	-3.38x + 39.71	0.99	0.00	ns	97.4%
<i>P. chesapeaki</i>	Gill	5	-3.44x + 40.18	0.98	0.15	ns	95.4%
<i>P. chesapeaki</i>	Gill	10	-3.50x + 41.89	0.94	0.65	ns	93.1%
<i>P. chesapeaki</i>	Gill	20	-3.36x + 42.12	0.95	0.01	ns	98.3%
<i>P. chesapeaki</i>	Digestive gland	2	-3.47x + 40.18	0.99	0.42	ns	94.0%
<i>P. chesapeaki</i>	Digestive gland	5	-3.53x + 40.52	1.00	1.01	ns	92.2%
<i>P. chesapeaki</i>	Digestive gland	10	-3.51x + 41.97	0.95	0.92	ns	92.5%
<i>P. chesapeaki</i>	Digestive gland	20	-3.39x + 41.97	0.96	0.01	ns	97.2%
<i>P. chesapeaki</i>	Adductor muscle	2	-3.43x + 39.94	0.99	0.12	ns	95.6%
<i>P. chesapeaki</i>	Adductor muscle	5	-3.41x + 40.03	0.99	0.06	ns	96.3%
<i>P. chesapeaki</i>	Adductor muscle	10	-3.09x + 40.84	0.85	5.47	*	110.5%
<i>P. chesapeaki</i>	Adductor muscle	20	-3.15 + 40.69	0.97	2.34	ns	107.8%
<i>P. chesapeaki</i>	Foot	2	-3.64x + 41.08	0.99	2.22	ns	88.3%
<i>P. chesapeaki</i>	Foot	5	-3.61x + 41.83	0.95	1.98	ns	89.3%
<i>P. chesapeaki</i>	Foot	10	-2.32x + 39.39	0.40	24.56	***	169.6%
<i>P. chesapeaki</i>	Foot	20	-3.37x + 42.98	0.98	16.08	***	98.2%
<i>P. chesapeaki</i>	Mantle	2	-3.53x + 40.80	0.99	4.60	ns	92.1%
<i>P. chesapeaki</i>	Mantle	5	-3.51x + 42.26	0.93	1.50	ns	92.6%
<i>P. chesapeaki</i>	Mantle	10	-2.15x + 38.31	0.45	11.29	**	192.3%
<i>P. chesapeaki</i>	Mantle	20	-2.75x + 42.59	0.89	12.46	***	130.8%
<i>P. chesapeaki</i>	Remaining tissue	2	-3.43x + 40.56	0.98	0.12	ns	95.7%
<i>P. chesapeaki</i>	Remaining tissue	5	-2.45x + 40.49	0.38	39.09	***	156.4%
<i>P. chesapeaki</i>	Remaining tissue	10	-2.80x + 42.53	0.64	5.65	*	127.4%
<i>P. chesapeaki</i>	Remaining tissue	20	-3.26x + 46.87	0.91	13.55	***	102.5%

References.

- Arzul. I., Chollet. B., Michel. J., Robert. M., Garcia. C., Joly. J.-P., François. C. and Miossec. L.** (2012). One *Perkinsus* species may hide another: characterization of *Perkinsus* species present in clam production areas of France. *Parasitology* **139**. 1757–1771. doi: 10.1017/S0031182012001047.
- Brown. G. D., Hudson. K. L. and Reece. K. S.** (2004). Multiple polymorphic sites at the ITS and ATAN loci in cultured isolates of *Perkinsus marinus*. *Journal of Eukaryotic Microbiology* **51**. 312–320. doi: 10.1111/j.1550-7408.2004.tb00572.x.
- Burreson. E. M., Reece. K. S. and Dungan. C. F.** (2005). Molecular, morphological, and experimental evidence support the synonymy of *Perkinsus chesapeaki* and *Perkinsus andrewsi*. *Journal of Eukaryotic Microbiology* **52**. 258–270. doi: 10.1111/j.1550-7408.2005.05-00035.x.
- Casas. S. M., Grau. A., Reece. K. S., Apakupakul. K., Azevedo. C. and Villalba. A.** (2004). *Perkinsus mediterraneus* n. sp., a protistan parasite of the European flat oyster *Ostrea edulis* from the Balearic Islands, Mediterranean Sea. *Diseases of Aquatic Organisms* **58**. 231–244. doi: 10.3354/dao058231.
- Casas. S. M., Reece. K. S., Li. Y., Moss. J. A., Villalba. A. and La Peyre. J. F.** (2008). Continuous culture of *Perkinsus mediterraneus*, a parasite of the European flat oyster *Ostrea edulis*, and characterization of its morphology, propagation, and extracellular proteins *in vitro*. *Journal of Eukaryotic Microbiology* **55**. 34–43. doi: 10.1111/j.1550-7408.2008.00301.x.

- Choi. K.-S., Wilson. E. A., Lewis. D. H., Powell. E. N. and Ray. S. M.** (1989). The energetic cost of *Perkinsus marinus* parasitism in oysters: quantification of the thioglycollate method. 125–131.
- da Silva. P. M., Vianna. R. T., Guertler. C., Ferreira. L. P., Santana. L. N., Fernández-Boo. S., Ramilo. A., Cao. A. and Villalba. A.** (2013). First report of the protozoan parasite *Perkinsus marinus* in South America, infecting mangrove oysters *Crassostrea rhizophorae* from the Paraíba River (NE, Brazil). *Journal of Invertebrate Pathology* **113**. 96–103. doi: 10.1016/j.jip.2013.02.002.
- da Silva. P. M., Scardua. M. P., Vianna. R. T., Mendonça. R. C., Vieira. C. B., Dungan. C. F., Scott. G. P. and Reece. K. S.** (2014). Two *Perkinsus* spp. infect *Crassostrea gasar* oysters from cultured and wild populations of the Rio São Francisco estuary, Sergipe, northeastern Brazil. *Journal of Invertebrate Pathology* **119**. 62–71. doi: 10.1016/j.jip.2014.04.005.
- Dungan. C. F. and Reece. K. S.** (2006). *In Vitro* propagation of two *Perkinsus* spp. parasites from Japanese Manila clams *Venerupis philippinarum* and description of *Perkinsus honshuensis* n. sp. *Journal of Eukaryotic Microbiology* **53**. 316–326. doi: 10.1111/j.1550-7408.2006.00120.x.
- Elandaloussi. L. M., Carrasco. N., Roque. A., Andree. K. and Dolores Furones. M.** (2009). First record of *Perkinsus olseni*, a protozoan parasite infecting the commercial clam *Ruditapes decussatus* in Spanish Mediterranean waters. *Journal of Invertebrate Pathology* **100**. 50–53. doi: 10.1016/j.jip.2008.09.004.

- Itoh. N., Meyer. G., Tabata. A., Lowe. G., Abbott. C. and Johnson. S.** (2013). Rediscovery of the Yesso scallop pathogen *Perkinsus qugwadi* in Canada. and development of PCR tests. *Diseases of Aquatic Organisms* **104**. 83–91. doi: 10.3354/dao02578.
- Moss. J. A., Xiao. J., Dungan. C. F. and Reece. K. S.** (2008). Description of *Perkinsus beihaiensis* n. sp., a new *Perkinsus* sp. parasite in oysters of southern China. *Journal of Eukaryotic Microbiology* **55**. 117–130. doi: 10.1111/j.1550-7408.2008.00314.x.
- Queiroga. F. R., Vianna. R. T., Vieira. C. B., Farias. N. D. and Da Silva. P. M.** (2015). Parasites infecting the cultured oyster *Crassostrea gasar* (Adanson, 1757) in northeast Brazil. *Parasitology* **142**. 756–766. doi: 10.1017/S0031182014001863.
- Ramilo. A., Carrasco. N., Reece. K. S., Valencia. J. M., Grau. A., Aceituno. P., Rojas. M., Gairin. I., Furones. M. D., Abollo. E. and Villalba. A.** (2015). Update of information on perkinsosis in NW Mediterranean coast: Identification of *Perkinsus* spp. (Protista) in new locations and hosts. *Journal of Invertebrate Pathology* **125**. 37–41. doi: 10.1016/j.jip.2014.12.008.
- Ramilo. A., Pintado. J., Villalba. A. and Abollo. E.** (2016). *Perkinsus olseni* and *P. chesapeaki* detected in a survey of perkinsosis of various clam species in Galicia (NW Spain) using PCR–DGGE as a screening tool. *Journal of Invertebrate Pathology* **133**. 50–58. doi: 10.1016/j.jip.2015.11.012.
- Reece. K., Dungan. C. and Burreson. E.** (2008). Molecular epizootiology of *Perkinsus marinus* and *P. chesapeaki* infections among wild oysters and clams in Chesapeake bay, USA. *Diseases of Aquatic Organisms* **82**. 237–248. doi: 10.3354/dao01997.

Reece. K. S., Scott. G. P., Dang. C. and Dungan. C. F. (2017). A novel monoclonal *Perkinsus chesapeaki* *in vitro* isolate from an Australian cockle. *Anadara trapezia*. *Journal of Invertebrate Pathology* **148**. 86–93. doi: 10.1016/j.jip.2017.05.007.

Sabry. R. C., Gesteira. T. C. V., Magalhães. A. R. M., Barracco. M. A., Guertler. C., Ferreira. L. P., Vianna. R. T. and da Silva. P. M. (2013). Parasitological survey of mangrove oyster. *Crassostrea rhizophorae*. in the Pacoti river estuary. Ceará state. Brazil. *Journal of Invertebrate Pathology* **112**. 24–32. doi: 10.1016/j.jip.2012.10.004.

Shamal. P., Zacharia. P. U., Binesh. C. P., Pranav. P., Suja. G., Asokan. P. K., Pradeep. M. A., Rithesh. R., Vijayan. K. K. and Sanil. N. K. (2018). *Perkinsus olseni* in the short neck yellow clam. *Paphia malabarica* (Chemnitz, 1782) from the southwest coast of India. *Journal of Invertebrate Pathology* **159**. 113–120. doi: 10.1016/j.jip.2018.10.001.

Valencia. J. M., Bassitta. M., Picornell. A., Ramon. C. and Castro. J. A. (2014). New data on *Perkinsus mediterraneus* in the Balearic archipelago: locations and affected species. *Diseases of Aquatic Organisms* **112**. 69–82. doi : 10.3354/dao02795.

Ye. J., Coulouris. G., Zaretskaya. I., Cutcutache. I., Rozen. S. and Madden. T. L. (2012). Primer-BLAST: A tool to design target-specific primers for polymerase chain reaction. *BMC Bioinformatics* **13**. 1–11. doi: 10.1186/1471-2105-13-134.

1 Duplex qPCR assay development

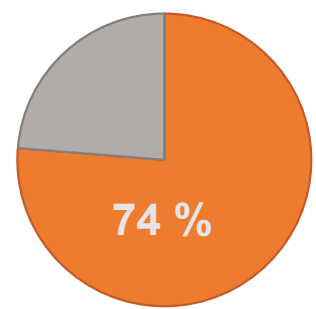


- Gill
- Digestive gland
- Mantle
- Foot
- Adductor muscles
- Remaining tissue

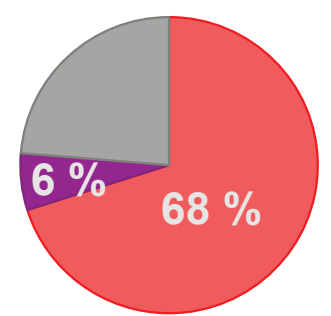
►► Presence of PCR inhibitors depending on organ-type

2 Comparison RFTM and qPCR methods

RFTM



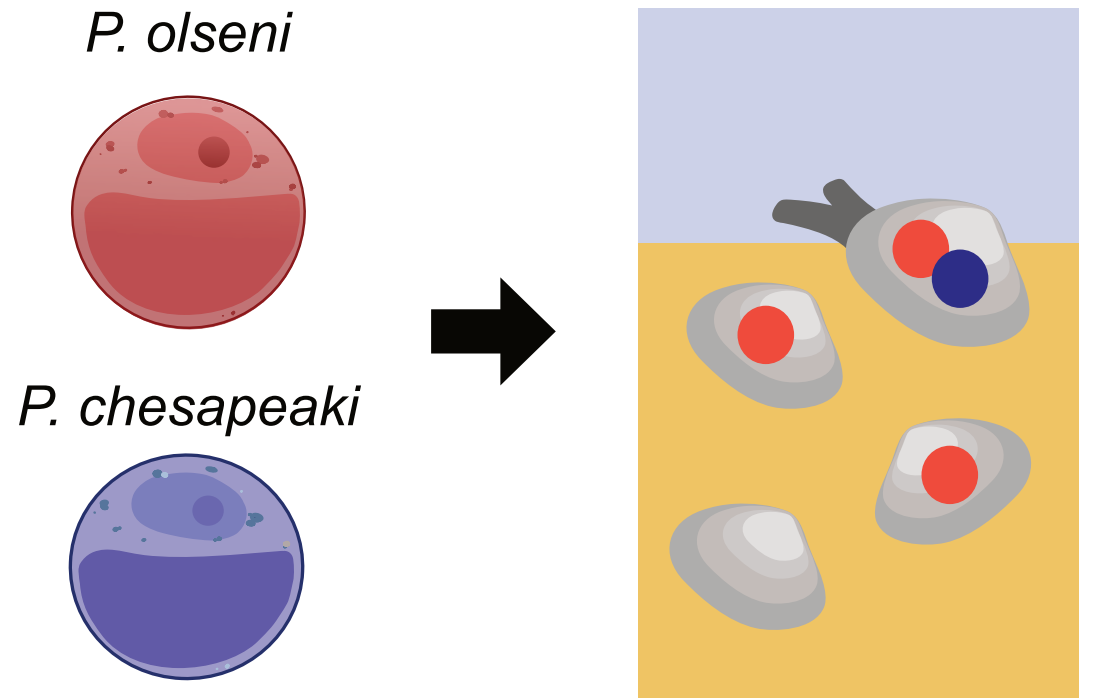
qPCR



- not infected
- Perkinsus* spp.
- P. olsenii* only
- Co-infected

►► RFTM and qPCR are complementary but only qPCR can quantify abundance at species level

3 *In situ* co-detection and quantification



►► Single-infection was only detected for *P. olsenii* parasite.

►► The infection intensities of co-infected organisms are dominated by *P. olsenii* parasite.